The origin and dynamics of nitrogen in the Earth's mantle constrained by 15N15N in hydrothermal gases

Jabrane Labidi, Edward Young

Invited Review article for *Chemical Geology*

The origin and dynamics of nitrogen in the Earth's mantle constrained by $^{15}N^{15}N$ in hydrothermal gases

J. Labidi[1], E.D. Young[2]

[1] Université de Paris, Institut de physique du globe de Paris, CNRS, Paris, France

[2] Department of Earth, Planetary, and Space Sciences, UCLA, Los Angeles, CA, USA.

7,285 words, 7 figures

Abstract

The development of high-resolution gas source mass spectrometry has permitted entirely new types of measurements of multiply-substituted isotopologues in gas species of geochemical significance. Here, we present recent advances afforded by measurements of $^{15}N^{15}N$ in natural samples, together with $^{14}N^{14}N$ and $^{15}N^{14}N$. We show that the abundance of the doubly-substituted $^{15}N^{15}N$ isotopologue in hydrothermal gases, often mixtures of volatiles of widely different origins, allows tracing the provenance of nitrogen. The approach is based on the recent finding that atmospheric N_2 has a substantial enrichment in $^{15}N^{15}N$ of nearly 20‰ relative to any other source of N_2. This is particularly useful for the study of hydrothermal gases, where characterizing the isotopic composition and provenance of volcanic N_2 is important for a wide range of applications in high-temperature geochemistry, but where air-derived N_2 is unavoidable. In this review, we summarize the evidence that $^{15}N^{15}N$ is an unambiguous tracer of air

contamination. We compare two sets of published $^{15}N^{15}N$ data acquired on gases from plume and arc volcanoes. We show how different sources of volcanic N_2 may be in plume versus arc environments, and discuss the first-order constraints on the deep N cycle that are provided by the new $^{15}N^{15}N$ data. Important findings include that the $\delta^{15}N$ tracer, used alone or in conjunction with N_2/Ar and N_2/He ratios, can be surprisingly deceiving. Isotope fractionation of atmospheric nitrogen occurs within hydrothermal systems, resulting in negative $\delta^{15}N$ values similar to estimates for mantle values, yet with $^{15}N^{15}N$ values that preclude a mantle origin. The $^{15}N^{15}N$ data show that the true $\delta^{15}N$ of volcanic components is positive in arcs but near-zero at the Yellowstone plume. In other words, atmospheric N_2 can mimic mantle $\delta^{15}N$, and mantle $\delta^{15}N$ can look like the value of air. Without $^{15}N^{15}N$, the apportioning of mantle and atmospheric N_2 in mixed gases can easily be wrong. With $^{15}N^{15}N$, we also determine the true $N_2/^3He$ and $N_2/^{36}Ar$ ratios of volcanic components in hydrothermal systems. Results inform our understanding of the deep nitrogen cycle. Plume and arc volcanic endmembers show distinct isotope and elemental ratios, consistent with sub-arc sources being overwhelmed by near-quantitative slab devolatilization, while the Yellowstone plume source is not reflecting volatile subduction.

1. Introduction

Plate tectonics has shuffled the record of volatiles acquired by Earth's mantle during planetary formation (Bekaert et al., 2021; Hilton et al., 2002; Jambon, 1994). Disambiguating the relative importance of subducted and primordial volatiles in the global budget of the deep Earth is crucial for a better understanding of planetary evolution. Information about the N isotopic composition of Earth's mantle comes partly from basalts: quenching during

48 eruption of mid-ocean ridge basalts (MORB) on the seafloor results in the formation of glassy
49 rims preserving magmatic vesicles enriched in volatiles. These vesicles are a potential
50 treasure trove for sampling mantle volatiles. However, because nitrogen is a trace gas in
51 those vesicles, magmatic nitrogen contained within them is commonly contaminated by N_2-
52 rich air-derived components upon eruption (Marty, 1995; Marty and Zimmermann, 1999).
53 One strategy to see through the contamination by air has been to determine nitrogen isotope
54 ratios together with $^{40}Ar/^{36}Ar$ ratios (Marty, 1995). The rationale is that air and the mantle
55 have distinct $^{40}Ar/^{36}Ar$ ratios, ~ 300 and ~ 25,000 respectively (Moreira et al., 1998). Basalts
56 with $^{40}Ar/^{36}Ar$ ratios ~ 300 similar to air show evidence for air-derived nitrogen, while lavas
57 with $^{40}Ar/^{36}Ar$ ratios greater than ~1,000 appear to exhibit $\delta^{15}N$[1] values closer to true
58 mantle values (Marty, 1995; Marty and Zimmermann, 1999). Based on basalt studies, a $\delta^{15}N$
59 value of ~ –4‰ relative to air may be adopted as an estimate for the convective mantle (data
60 in Barry and Hilton, 2016; Cartigny et al., 2001; Javoy and Pineau, 1991; Marty, 1995; Marty
61 and Humbert, 1997; Marty and Zimmermann, 1999). Nitrogen in Earth's mantle is therefore
62 isotopically distinct from solar ($\delta^{15}N$ ~ –400‰, Hashizume et al., 2000; Marty et al., 2011)
63 and from potential chondritic sources akin to enstatite chondrites ($\delta^{15}N$ ~ –20‰ Grady et
64 al., 1986). The clear disagreement between mantle nitrogen and potential primordial
65 signatures has been suggested to reflect subduction of surface derived N with elevated $\delta^{15}N$
66 values, resulting in the departure from enstatite chondrites and/or solar $\delta^{15}N$ values
67 towards higher $\delta^{15}N$ over time (Barry and Hilton, 2016; Javoy, 1998; Marty and Dauphas,
68 2003; Williams and Mukhopadhyay, 2018). In other words, vestiges of primordial nitrogen

[1] $\delta^{15}N$ refers to the per mil deviations in $^{15}N/^{14}N$ from the ratio in air.

acquired during Earth's accretion would have been erased with time by ongoing plate tectonics. One requirement of this scenario is that surface nitrogen must have had $\delta^{15}N >$ 20‰ in the Hadean and Archean, so that it can balance extremely low $\delta^{15}N$ for the primordial mantle (Javoy, 1998). The consistently high $\delta^{15}N$ values in deep time are simply not observed (Ader et al., 2016; Marty et al., 2013; Pinti et al., 2001), leaving the nitrogen deep cycle unexplained.

Constraining the nitrogen isotopic compositions of the sources of mantle plumes and arc volcanoes should help. Mantle plumes host primordial gases, undisturbed and isolated from mantle convection for nearly 4.4 Gy, mixed with subducted components (Mukhopadhyay, 2012; Parai et al., 2019). Plume basaltic glasses are however far less available than MORB, and therefore less well understood. Only seven plume basalts with $^{3}He/^{4}He$ ratios > 16 and published $\delta^{15}N$ values pass the tests of having avoided complete volatile overprinting by air contamination (i.e., non-air $^{40}Ar/^{36}Ar$ ratios). Those samples have $\delta^{15}N$ values between –2‰ and 0‰ (data in Marty and Dauphas, 2003; Marty and Humbert, 1997; Sano et al., 2001), marginally higher than the convective mantle. Given the paucity of data, the influence of subduction on the N budget of mantle plumes remains unclear. Nitrogen in arc mantle sources is also important to study, as it is likely influenced by recycled surface-derived components (Fischer et al., 2002; Füri et al., 2021; Taran, 2009). Sub-arc nitrogen may be especially well suited for placing constraints on N isotope signatures that may be transferred to the deep Earth. However, the N isotope compositions of sub-arc sources are even more challenging to constrain because no glasses are available for analysis.

The study of volcanic gases offers a unique window into plumes and arc volatiles where glasses are rare or absent. A large array of hot springs and fumaroles are vented to the

surface and reflect mixtures between surface waters, atmospheric gases, and variable amounts of volcanic volatiles (Giggenbach, 1992). Instances of vented gases with plume-like $^{3}He/^{4}He$ ratios are associated with $^{40}Ar/^{36}Ar$ ratios that remain under 1,000 (Boudoire et al., 2020; Caliro et al., 2015; Chiodini et al., 2012; Sano et al., 1985). This is much lower than the values of ~ 5,000 to 10,000 thought to characterize the deep mantle (Mukhopadhyay, 2012; Trieloff et al., 2000). Low $^{40}Ar/^{36}Ar$ in vented gases likely reflects a pattern of even greater air contamination than evidenced in basalts. Gases emitted by arc volcanoes are also heavily studied, but so far have shown $^{40}Ar/^{36}Ar$ ratios that are almost exclusively atmospheric (Hilton et al., 2002; Pedroni et al., 1999; Sano and Fischer, 2013; Snyder et al., 2001). It is unclear whether this reflects even more pronounced contamination directly from air, or instead results from volcanic sources overwhelmed by subducted air-derived argon (Staudacher and Allègre, 1988). In summary, gases from both plumes and arcs appear dominated by atmospheric $^{40}Ar/^{36}Ar$ signatures, which is problematic for the identification of volcanic N_2 in the gas mixtures.

As an alternative to relying on $^{40}Ar/^{36}Ar$ measurements alone as tracers of air contamination, studies of fumaroles have often employed plots of $\delta^{15}N$ values versus bulk N_2/Ar and N_2/He ratios, in part because these gas species ratios are easy to measure with ordinary gas chromatography and quadrupole mass spectrometry techniques. In principle, N_2/Ar and N_2/He ratios should allow the identification of mixing between mantle and atmospheric endmembers, since air and various mantle sources are anticipated to be very different (Elkins et al., 2006; Fischer et al., 2002, 1998; Roulleau et al., 2013; Sano et al., 2001, 1998; Taran, 2009; Zimmer et al., 2004). By design, the approach relies on the assumption that $\delta^{15}N$, N_2/He and N_2/Ar ratios remain unfractionated, and are thus strictly tracers of

115 mixing in hydrothermal systems. Some of the most notable and vexing observations to date
116 using this method include: (1) various sub-arc regions show consistently positive $\delta^{15}N$ at
117 relatively high N_2/He and N_2/Ar ratios (Elkins et al., 2006; Fischer et al., 2002; Taran, 2011,
118 2009); (2) rare but remarkable occurrences of MORB $\delta^{15}N$ signatures in some arc volcanoes
119 (Fischer et al., 2002; Zimmer et al., 2004); (3) plume gases at Yellowstone with elevated
120 $^3He/^4He$ ratios and $\delta^{15}N$ values clustered around 0‰, the value of air, even at N_2/He ratios
121 five orders of magnitude below the value of the atmosphere (Chiodini et al., 2012); and (4)
122 other plume gases, from both Iceland and Azores, also with elevated $^3He/^4He$ but higher
123 N_2/He (i.e., closer to air) and negative $\delta^{15}N$ values as low as –10‰, nominally inconsistent
124 with the signature of contaminant air (Caliro et al., 2015; Marty et al., 1991; Sano et al., 1985).
125 In the latter case, the surprisingly low $\delta^{15}N$ values were interpreted as either reflecting a
126 unique feature of the high $^3He/^4He$ mantle, resembling of the values for enstatite chondrites
127 (Caliro et al., 2015; Marty et al., 1991) or as the result of N isotopic fractionation of
128 atmospheric N_2 in the hydrothermal systems (Marty et al., 1991). Overall, it is hard to
129 reconcile $\delta^{15}N$ values with high $^3He/^4He$ from one site to another. What is clear from this
130 brief literature review is that the nitrogen isotope geochemistry of hydrothermal fluids is
131 potentially of great utility for constraining the cycle of nitrogen in the deep Earth, but simple
132 conclusions are hindered by pervasive air contamination.

133 The burgeoning field commonly referred to as “clumped” isotope geochemistry makes
134 use of the relative abundance of multiply-substituted isotopologues in a given molecule, i.e.,
135 the abundance of isotopic molecular species with more than one heavy isotope substitution
136 (hence the term “clumping” of isotopes). A number of molecules have been investigated,
137 although studies of rare isotopologues of CO_2 and CH_4 dominate the field. The main goal in

138 many of these studies has been to derive temperatures of formation of carbonate minerals
139 (in the case of CO_2 liberated from carbonates) or the origins of various gases, with an
140 emphasis on the potential biogenicity of the gases in the case of CH_4 (Henkes et al., 2018;
141 Young et al., 2017). Here we describe a somewhat different application in which isotope
142 clumping is a unique tracer of provenance, in this case $^{15}N^{15}N$ in N_2 gas in volcanic systems.
143 This tracer arises because of an extraordinary disequilibrium overabundance of $^{15}N^{15}N$ in
144 air. In this review, we summarize work to date that illustrates how the $^{15}N^{15}N$ novel tracer
145 places new constraints on air contamination of hydrothermal samples (Labidi et al., 2021,
146 2020; Yeung et al., 2017). We present observations and constraints from our recent studies
147 of the rare isotopologue $^{15}N^{15}N$ in nitrogen from hydrothermal gases worldwide,
148 representing both plumes and arcs. Recently published $^{15}N^{15}N$ data offer a distinctive
149 perspective on nitrogen recycling in these various geodynamic settings. We summarize the
150 evidence that the new $^{15}N^{15}N$ tracer is an unambiguous indicator of air contamination for
151 nitrogen, much more so than $\delta^{15}N$ alone, $^{40}Ar/^{36}Ar$ ratios, or even $\delta^{15}N$ associated with N_2/He
152 and N_2/Ar ratios. In this review, we discuss new evidence that $\delta^{15}N$ and N_2/Ar fractionations
153 are at play in hydrothermal systems. We identify the composition of volcanic N_2 in the plume
154 and arc environments, and discuss the first-order constraints on the deep N cycle that are
155 provided by the new $^{15}N^{15}N$ data.
156
157 **2. $^{15}N^{15}N$: an air tracer *par excellence***
158 The doubly-substituted isotopologue $^{15}N^{15}N$ is an example of a "clumped" isotopic
159 species, a term often invoked in the geochemical literature to describe isotopic molecular
160 species (isotopologues) with more than one heavy isotope. The application of $^{15}N^{15}N$ to

tracing the provenance of volcanic gases is based on the recent discovery that atmospheric nitrogen possesses a considerable $^{15}N^{15}N$ enrichment of nearly 2% (Yeung et al., 2017), making air easy to distinguish from any magmatic nitrogen or nitrogen produced by other geochemical or biological processes. In the laboratory, we measure $^{29}N_2/^{28}N_2$ and $^{30}N_2/^{28}N_2$ ratios and report them as $\delta^{29}N_2$ and $\delta^{30}N_2$, the per mil deviations from air. In the case of $^{29}N_2/^{28}N_2$ $\delta^{29}N_2 = 1000\times((^{29}R_{sample}/^{29}R_{air} - 1)$ (‰) where $^{29}R=(^{14}N^{15}N+^{15}N^{14}N)/^{14}N^{14}N$ for the gas of interest. Since $(^{14}N^{15}N+^{15}N^{14}N)/^{14}N^{14}N$ equals $2(^{15}N/^{14}N)$ for both the sample and the standard, for all practical purposes, $\delta^{29}N_2$ is equivalent to the bulk isotope ratio expressed as $\delta^{15}N = 1000 \times (^{15}R_{sample}/^{15}R_{air} - 1)$. For $^{30}N_2/^{28}N_2$, $\delta^{30}N_2 = 1000\times(^{30}R_{sample}/^{30}R_{air} - 1)$ (‰) where $^{30}R=^{15}N^{15}N/^{14}N^{14}N$ for a given sample. In general, simple fractionation by molecular weight of N_2 will result in variations in $\delta^{30}N_2$ that are roughly twice the variations in $\delta^{29}N_2$ (see below).

The Δ_{30} tracer is a measure of departures from a purely stochastic distribution of ^{15}N and ^{14}N atoms comprising the isotopic molecular species. It is defined such that $\Delta_{30} = 1000\times(^{30}R/(^{15}R)^2-1)$ (‰), where $^{15}R=^{15}N/^{14}N$ for the gas of interest. The value $(^{15}R)^2$ represents the stochastic relative abundance of $^{30}N_2$, and reflects the fact that the probability of forming $^{30}N_2$ from a purely random distribution of ^{14}N and ^{15}N atoms across all nitrogen isotopologues is the square of the probability of finding molecules with just one ^{15}N (concentrations are in effect probabilities in the stochastic limit). Of course, the formation of $^{15}N^{15}N$ is not necessarily purely random. The low vibrational energy of this doubly-substituted molecule results in a thermodynamic driving force for its formation. The thermodynamic favorability for $^{15}N^{15}N$ formation is strongest at the lower temperatures. At geochemically relevant temperatures ranging from 200 to 1000 °C, equilibrium among N_2

184 isotopologues results in Δ_{30} values from 0.5 to 0.1‰, respectively (Yeung et al., 2017). This
185 applies for any N_2 molecule made in a geological process, whether it is mantle-derived or
186 inherited from slabs, for example (Labidi et al., 2020).

187 In contrast to expectations from equilibrium thermodynamics and normal, purely mass-
188 dependent fractionation processes, air has a pronounced disequilibrium enrichment in
189 $^{15}N^{15}N$, leading to an atmospheric Δ_{30} value of 19.1±0.3‰ (2σ) (Yeung et al., 2017). The Δ_{30}
190 value of air behaves as an indelible signature that is an isotopologue (molecular) analogue
191 of the three-isotope anomaly that has proven so useful in oxygen isotopes, $\Delta^{17}O$ (e.g., Clayton
192 and Mayeda, 1984): it is not erased by mass-dependent fractionation of N_2 and is not re-
193 ordered in heated hydrothermal systems (see appendix C). The use of Δ_{30} as a tracer of air
194 does not require any assumptions about the relative abundances of other tracers, as is the
195 case for $^{40}Ar/^{36}Ar$ or N_2/Ar ratios. Instead, we use the isotopic compositions of the N_2
196 molecules themselves to trace the origin of the nitrogen in a manner that is more diagnostic
197 than $\delta^{15}N$. Based on the application of this tracer to volcanic hydrothermal systems, we show
198 that both $\delta^{15}N$ and N_2/Ar experience fractionations in natural hydrothermal systems, and
199 that atmospheric-like $^{40}Ar/^{36}Ar$ ratios may be genuine features of the sub-arc mantle.
200 Ultimately, previously unrecognized fractionation of $^{15}N/^{14}N$ (expressed as shifts in $\delta^{15}N$)
201 and N_2/Ar appear to have conspired to produce deceptive indicators for the origin of N in
202 gas mixtures that Δ_{30} measurements can help rectify.

203 In what follows we illustrate the potency of $^{15}N^{15}N$ to constrain the true $\delta^{15}N$, $N_2/^{36}Ar$,
204 $N_2/^{3}He$, $^{40}Ar/^{36}Ar$, and even $^{3}He/^{36}Ar$ ratios of volcanic components contributing to
205 hydrothermal gases. The new $^{15}N^{15}N$ data offer valuable constraints on the deep-Earth cycles

206 of both nitrogen and argon, especially when associated with conventional noble gases
207 measurements.
208
209 **3. Measurements of isotope ratios at high mass resolution: the challenge of**
210 **$^{15}N^{15}N$**
211 Measurements of nitrogen isotopologues involve high-mass-resolution mass
212 spectrometry. The abundances of $^{14}N^{14}N^+$, $^{14}N^{15}N^+$ (representing both isotopomers, $^{14}N^{15}N$
213 and $^{15}N^{14}N$) and $^{15}N^{15}N^+$ ions are measured with high mass resolution to avoid mass-to-
214 charge interferences. Interferences for $^{28}N_2$ ($^{14}N^{14}N^+$) and $^{29}N_2$ ($^{14}N^{15}N^+$) are from carbon
215 monoxide, ^{28}CO ($^{12}C^{16}O^+$) and ^{29}CO ($^{13}C^{16}O^+$ and $^{12}C^{17}O^+$). The $m/\Delta m$ separating ^{28}CO
216 ($^{12}C^{16}O^+$) from $^{28}N_2$ ($^{14}N^{14}N^+$) is ~2,500, while values of ~6,000 and ~7,000 separate $^{13}C^{16}O^+$
217 and $^{12}C^{17}O^+$ from $^{29}N_2^+$, respectively. Based on the zero-order rule that mass resolving power
218 (instrumental $m/\Delta m$) must be ~ 3 x $m/\Delta m$ between the species, mass resolving powers of at
219 least 7,500, 18,000 and 21,000, respectively, are required to separate N_2 from interferences
220 on nominal masses 28 and 29. In the case of mass/charge 30, low backgrounds of nitrogen
221 monoxide (NO^+) are ubiquitous and require a sufficiently high mass resolution to separate
222 $^{30}NO^+$ from $^{30}N_2^+$. The $m/\Delta m$ between $^{30}NO^+$ and $^{30}N_2^+$ is ~13,400, requiring an instrumental
223 mass resolving power of at least ~45,000.
224 At the time of this writing, and to the best of our knowledge, $^{30}N_2$ measurements have
225 been performed only at the University of California, Los Angeles (UCLA) on a *Nu Instruments*
226 Panorama. Routine measurements at mass resolving powers above 50,000 are achieved with
227 an entrance slit width of about 30 μm. A mass spectrum of the $^{30}N_2^+$ beam under working
228 conditions is shown in Young et al. (2016). $^{30}N_2^+$ ions are detected using a secondary electron

multiplier, with count rates of between 5,000 and 40,000 cps for most natural samples. Ions with m/z of 28 and 29 are measured using Faraday cups with 10^{11} Ω amplifier resistors.

Natural samples from the field show a broad range of N_2 concentrations, typically from 0.01 vol% N_2 to 80 vol% N_2. These concentrations translate into between 1 and 500 μmoles of N_2 for published Δ_{30} analyses. Counting times are adjusted to account for the large range in sample N_2 concentrations. This results in variable analytical precision from one sample to another. Samples yielding ≥ 5 μmoles of N_2 permit conventional dual-inlet measurements, with analysis times of up to 7.5 hours to yield the best precision. For samples with < 5 μmoles of N_2, measurements have been performed by concentrating on a liquid-nitrogen "microvolume", with analysis times of 1 hour at most. For analyses lasting 7.5 hours, internal precision for Δ_{30} values is typically ≤0.2‰ (1 s.e.). Samples with less than 5 μmoles N_2 yield internal uncertainties of between 0.18 and 1.80‰ (1 s.e.).

4. $^{15}N^{15}N$ composition of N_2 in nature

The published data for natural samples for which we have obtained Δ_{30} values are from Yeung et al., (2017), Labidi et al. (2020) and Labidi et al. (2021). They are shown in a plot of $\delta^{29}N_2$ versus $\delta^{30}N_2$ in Fig. 1 and as Δ_{30} versus $\delta^{15}N$ in Fig. 2. Published data summarized here include samples of air N_2, as well as magmatic, hydrothermal and crustal gases (see Yeung et al. 2017 for analyses of biologically-produced N_2 which have Δ_{30} values within ~1 ‰ of zero). The dataset is dominated by hydrothermal samples (n=48) but also features measurements of magmatic (n=4, MORB in figure 1) and crustal fluids (n=5, mine gases in figure 1). Magmatic samples were extracted from mid-ocean ridge basalts with high volatile content (n=4). Crustal gases are extracted from fractures at depth, from the Canadian shield

(n=5). Hydrothermal samples are from plumes and arcs from Halemaumau (n=1, Hawaii), various locations within Iceland (n=11), the Yellowstone caldera (n=13, USA), the Eifel region (n=5, Germany), and the Momotombo (n=2, Nicaragua), Santa Ana (n=1, El Salvador), and Poás (n=5, Costa Rica) volcanos as well from an array of springs from Costa Rica and Panama (n=6).

The data reveal patterns dominated by the presence or absence of the atmospheric Δ_{30} signature. In Fig. 1, correlated variations of $\delta^{30}N_2$ against $\delta^{29}N_2$ are observed on two parallel lines with slopes of ~2, as expected where fractionation by molecular mass occurs. The upper line corresponds to air and samples fractionated from air, and the lower line includes samples unrelated to air that have equilibrium (or near equilibrium) concentrations of $^{15}N^{15}N$. The slope of ~2 results from the mass differences between $^{30}N_2$, $^{29}N_2$, and $^{28}N_2$. For example, diffusion of these molecules would lead to fractionation factors $\alpha_{29/28}$ and $\alpha_{30/28}$ (e.g., $\alpha_{29/28}=(^{29}N_2/^{28}N_2)_{diffused}/(^{29}N_2/^{28}N_2)_o$) for $^{29}N_2/^{28}N_2$ and $^{30}N_2/^{28}N_2$ of $\sqrt{(m^{28}N_2/m^{29}N_2)}$ and $\sqrt{(m^{28}N_2/m^{30}N_2)}$, respectively (Graham's law), where $m^{28}N_2$ is the molecular mass of $^{28}N_2$, and so forth. In general, $\alpha_{29/28} = \alpha_{30/28}^{\beta}$ where in this case $\beta = \ln(m^{28}N_2/m^{30}N_2)/\ln(m^{28}N_2/m^{39}N_2) = 0.5085$ (Young et al., 2002). Because shifts in delta values are related to fractionation factors by $\delta-\delta_o \sim 10^3 \ln(\alpha)$,the slope relating variations in $\delta^{30}N_2$ to $\delta^{29}N_2$ in Fig. 1 is $\sim 1/\beta$ or 1.966. Various examples of mixtures plot between the two lines.

The two lines are separated by the ~19‰ offset for air (Fig. 1). Gases heated in the laboratory between 400 and 1,000 °C reflect equilibrium bond-ordering with values of Δ_{30} near zero. We take the gases at 1,000 °C that plot on the lower line as useful representatives of the stochastic distribution of N_2 isotopologues. Figure 1 underscores the striking nature of the anomalous $^{30}N_2$ in air; temperatures ranging from 25 to 1000 °C should result in

275 Δ_{30} values from 1.1 to 0.1‰, respectively (Yeung et al., 2017). The ~19‰ disequilibrium
276 $^{15}N^{15}N$ excess for atmospheric N_2 is likely due to nitrogen photochemistry in the modern
277 upper atmosphere (Yeung et al., 2017). The mechanism responsible for the enrichment
278 evidently requires the presence of O_2 during N_2 photolysis, so predictions could be made for
279 planetary atmospheres containing N_2 but no O_2, including Earth's atmosphere prior to the
280 great oxygenation event. Most importantly for this review, the $^{15}N^{15}N$ enrichment in air is an
281 unambiguous measure of air in mixed gases.

282 Analysis of a variety of natural samples of nitrogen show mass fractionation of
283 molecular species is rife, as evidenced by slope-2 variability in $\delta^{30}N_2$ vs. $\delta^{29}N_2$ space (Fig. 1).
284 Importantly for this work on volcanic hydrothermal systems, the array of mass-dependent
285 signatures going through air indicates air-derived N_2 experiences mass fractionation in
286 nature. This is an important observation; nitrogen derived from air does not have a single
287 $\delta^{29}N$ (or $\delta^{15}N$) because N_2 can be fractionated by molecular mass. The mass fractionation
288 array defined by gases with equilibrium, or nearly equilibrium, Δ_{30} values result from
289 fractionation during geological and/or biological processing (Fig. 1).

290 In figure 2, Δ_{30} values are plotted against $\delta^{29}N_2$. Because $\delta^{29}N_2$ is numerically equal to
291 $\delta^{15}N$, all plots going forward directly use the $\delta^{15}N$ notation instead of $\delta^{29}N_2$. N_2 may be
292 produced during volcanic degassing, but also during metamorphism or thermogenic
293 cracking. Δ_{30} values of ~ 0‰ are expected for N_2 molecules from magmas because at high
294 temperatures, thermodynamic equilibrium approaches the random distribution of $^{15}N^{15}N$
295 relative to other N_2 isotopologues. This was verified by the study of mid-ocean ridge basalts
296 with extraordinarily high volatile concentrations. Crushing experiments under vacuum
297 released N_2 with Δ_{30} values between +1.2±2.6‰ and +3.0±3.6‰ (Fig. 2, Labidi et al., 2020).

These data confirm that magmatic N_2 formed by degassing at ~ 1200 °C has Δ_{30} ~ 0‰. The mechanism for N_2 formation in crustal environments is breakdown of NH_4–bearing phyllosilicates at peak metamorphic temperatures (Li et al., 2021). Gases from two deep mines in the Canadian shield have Δ_{30} values between 1.1±0.4‰ and 0.5±0.2‰ (2 σ, n=2). These data confirm that crustal generation of N_2 by metamorphism has Δ_{30} values < 1‰ as expected for approaches to thermodynamic equilibrium.

5. The Δ_{30} – $\delta^{15}N$ evidence that air is ubiquitous and fractionated

By way of summary, we can say that high-temperature N_2 is characterized by Δ_{30} of ~0‰ and variable $\delta^{15}N$, and that air-derived N_2 has a Δ_{30} value of 19‰ and can also have variable $\delta^{15}N$ (Fig. 2). A number of samples exhibit Δ_{30} values intermediate between air and stochastic. Because there is no primary mechanism for producing intermediate values, these samples must be mixtures between air and high-temperature, volcanic N_2 (see appendix C for evidence against Δ_{30} re-ordering in nature). In principle, mixing between two N_2 gases with very different $\delta^{15}N$ values but similar, near-equilibrium Δ_{30} values can produce anomalously high Δ_{30} values (i.e., mixing relationships are curves, not straight lines). In practice however, the differences in $\delta^{15}N$ values required to produce mixing curves with sufficient curvature to cause discernible aberrations in Δ_{30} are on the order of hundreds of permil (Yeung et al., 2017 – also, see appendix).

Because mixing in Δ_{30} – $\delta^{15}N$ space is effectively linear, it is straightforward to identify endmember N_2 compositions for mixtures. For hydrothermal samples with Δ_{30} values of 19‰, virtually all N_2 in the gas mixture is derived from air. Atmospheric Δ_{30} values dominate

most (but not all) hot spring data. This likely reflects the recharge of surficial hydrothermal systems by air-saturated meteoric fluids, causing atmospheric N_2 to dominate over high-temperature N_2. Gases from Iceland, the Yellowstone caldera, and the Poás volcano all show atmospheric Δ_{30} values but negative $\delta^{15}N$ down to –10‰ (Fig. 3). The negative $\delta^{15}N$ values are deceptively similar to the MORB value of –4±2‰ (Javoy and Pineau, 1991, Marty et al., 1999), but the Δ_{30} values preclude a magmatic origin. The negative $\delta^{15}N$ signatures must result from isotopic fractionation of air. The distribution of $\delta^{29}N_2$ and $\delta^{30}N_2$ along a slope of ~2 in Fig. 1 indicates mass fractionation of the air-derived nitrogen. The fractionation likely occurs in the sub-surface, after air-saturated meteoric waters feed atmospheric nitrogen into hydrothermal systems. Upon heating, fluids undergo water/gas partitioning, eventually resulting in volatile losses. If water/gas exchange is associated with a $^{15}N/^{14}N$ fractionation, the degassed fluids would have $^{15}N/^{14}N$ ratios ($\delta^{15}N$ values) distinct from that of the residual N_2 left in the geothermal waters. Air with $\delta^{15}N$ values between –5 and –10‰ indicate two alternative possibilities:

(1) N isotope fractionation factors are similar to Graham's law, resulting in the instantaneous release of N_2 greatly depleted in ^{15}N, while residual N_2 is enriched in ^{15}N, depending on the extent of degassing; or

(2) N isotope fractionations are smaller than suggested by Graham's law, but amplified by open-system Rayleigh distillations, in which both the product and the residue of the water/gas fractionation are drawn to low $\delta^{15}N$ as the proportion of N held by the aqueous phase decreases.

In case 1, where fractionation occurs as a single-step process, the fractionation factor for isotopologue partitioning could be as great as the inverse of the square root of the inverse

of the isotopologue mass ratio, which would result in $\delta^{29}N_2$ (or $\delta^{15}N$) for the effusing gas that is –17 ‰ lower than that of the aqueous phase. The residual nitrogen in the fluid would have a complimentary enriched $\delta^{29}N_2$ (or $\delta^{15}N$) value. By simply propagating a 17‰ fractionation between dissolved and exsolved N_2, one expects the low $\delta^{15}N$ of –6‰ seen in the Iceland dataset from Labidi et al., (2020) to eventually produce the complimentary high $\delta^{15}N$ values of +11‰, but these are not seen. The most positive $\delta^{15}N$ at an atmospheric Δ_{30} is only +0.5‰ in Icelandic fumaroles (Fig. 3). A single-step process therefore seems unlikely, and this is supported by experiments. The $^{15}N/^{14}N$ isotope fractionation between N_2 gas and N_2 dissolved in aqueous fluid, $\alpha = (^{29}R)_{gas}/(^{29}R)_{fluid}$, when expressed as $\delta^{15}N_{gas} - \delta^{15}N_{fluid}$, is found to range from –0.9 to +0.4 ‰ from 6 to 60 °C (Lee et al., 2015). The reversal of the fractionations at 40 °C indicates the N_2 isotope fractionation factors result from a kinetic rather than an equilibrium process, and that the kinetic fractionation is fundamentally different from the simple square-root of the inverse mass ratio. Above 40 °C, isotopically light N_2 is preferentially partitioned into the aqueous fluid phase, and isotopically heavy N_2 resides in the gaseous phase (Lee et al., 2015). Linear extrapolation to 100 °C results in a fractionation of +1.0‰. With this fractionation, Rayleigh distillation would push the product and the residue to $\delta^{15}N$ values as low as –5‰ and –6 ‰, for gas and fluid, with ~ 99% N_2 degassing. The possibility of a higher fractionation would change the exact fractions of degassed nitrogen, but would not fundamentally modify our main hypothesis: N_2 isotope fractionations in hydrothermal systems are to be expected as the result of significant degassing in the absence of meteoric, air-saturated water recharge.

There is also evidence that the fractionations of $\delta^{15}N$ in air-derived N_2 are variable on human timescales. In Iceland, fractionated air was observed with $\delta^{15}N$ values as low as –6‰

366 for gases sampled in 2018 (Labidi et al., 2020). Fumaroles sampled elsewhere in Iceland in
367 1982 (Sano et al., 1985) had $\delta^{15}N$ values down to –10‰ (Marty et al., 1991). At Poás,
368 fumaroles sampled between 1998 and 2001 produced unfractionated air with $\delta^{15}N = 0$ ‰
369 (Vaselli et al., 2003), while field expeditions a few months later in 2001, and in 2006–2007,
370 the same fumaroles yielded negative $\delta^{15}N$ values of —3‰ (Fischer et al., 2015, 2002;
371 Zimmer et al., 2004). The latter samples tend to have atmospheric Δ_{30} values (Labidi et al.,
372 2021), demonstrating the negative $\delta^{15}N$ are due to fractionation of atmospheric N_2.
373 Similarly, at Yellowstone, a field expedition in September 2007 (Chiodini et al., 2012) yielded
374 no measurable $\delta^{15}N$ fractionation. Samples taken in August 2018 in the same hydrothermal
375 vents resulted in greatly fractionated air signatures with $\delta^{15}N$ as low as ~ –10‰ (Labidi et
376 al., 2020). The $\delta^{15}N$ variability of air-derived N_2 should be a subject of future dedicated
377 studies. The time variability of $\delta^{15}N$ in N_2 derived from air in hydrothermal systems is
378 particularly problematical for using $\delta^{15}N$ as a tracer for the provenance of N_2. In the interim,
379 very negative $\delta^{15}N$ in hydrothermal systems should be regarded as a natural consequence of
380 degassing in the context of intermittent meteoric (air-saturated) water recharge. In all cases,
381 $\delta^{15}N$ alone in hydrothermal gases is a poor tracer of the origin of N_2. In the absence of $^{15}N^{15}N$
382 data, $\delta^{15}N$ alone may lead to erroneous conclusions regarding the origin of volatiles in
383 hydrothermal gases.
384
385 **6. Identifying high-temperature N_2**
386 Gases from Yellowstone, Eifel, and Central America all incorporate some high-
387 temperature N_2 with $\Delta_{30} \sim 0$, resulting in variable Δ_{30} values due to mixing with air.

Extrapolation of trends in data to Δ_{30} = 0 ‰ constrains the volcanic endmembers for $\delta^{15}N$ (Fig. 3), $N_2/^3He$ (Fig. 4), $N_2/^{36}Ar$ (Fig. 5) and $^{40}Ar/^{36}Ar$ (Fig. 6). Some of the main conclusions on high-temperature volatiles are summarized in a cartoon on Fig. 7.

Eifel gases happen to be the simplest to interpret of the entire Δ_{30} dataset because they have Δ_{30} values as low as 0.3±0.7‰, i.e., within uncertainty of 0‰, requiring no extrapolation whatsoever to determine the $\delta^{15}N$ of high-temperature N_2. For those gases, the high-temperature $\delta^{15}N$ value is –1.2±0.5‰, a value that is slightly higher than estimates for the average for MORB mantle of ~—4±2‰ (Javoy and Pineau, 1991; Marty and Zimmermann, 1999). This marginally higher value could indicate the addition of recycled nitrogen with positive $\delta^{15}N$ in the Eifel mantle source (Labidi et al., 2020).

At Poás and Momotombo, two volcanoes from Central America, Δ_{30} values range down to +3.4±1.0 and 1.5±0.3‰. Extrapolation of the linear fits to Δ_{30} values of zero suggests that the volcanic N_2 at Poás and Momotombo have $\delta^{15}N$ values of ~+1±0.5‰ and ~+5±0.5‰ respectively (Labidi et al., 2021). It is unclear whether the Poás endmember reflects a unique volcanic endmember across central America, or a fractionated value, disconnected from the magmatic signature (Labidi et al., 2021). Overall, in view of the expectation that slab-derived nitrogen should have $\delta^{15}N$ values of near + 5‰ (Busigny et al., 2011; Li and Bebout, 2005), these high-T estimates are consistent with the addition of recycled N in the central American sub-arc mantle.

For Yellowstone, the Δ_{30} values range down to 3.8±1.7‰, but the $\delta^{15}N$-Δ_{30} scatter is substantial (Fig. 3). An extrapolation of the $\delta^{15}N$-Δ_{30} data to Δ_{30} = 0 was carried out by Labidi et al., (2020) using only the data comprising the steep negative sloping array, resulting in an

estimate for volcanic $\delta^{15}N$ of +3±2‰ (Labidi et al., 2020). Given the magnitude of the $\delta^{15}N$-Δ_{30} scatter, it is unclear whether this extrapolation is valid. The alternative, more conservative approach is to use the sample with the lowest Δ_{30} to define a minimum $\delta^{15}N$ of~+0.2‰. Higher values suggested by Labidi et al., (2020) are possible, but are not required by the data as a whole on Fig. 3. We note that a high-temperature endmember with $\delta^{15}N$~ 0‰ is consistent with the data from Chiodini et al., (2012) for Yellowstone, perhaps lending support for the more conservative approach.

Overall, based on our Δ_{30} values from the fumaroles sampled thus far, we find high $\delta^{15}N$ in high-temperature components compared to MORB nitrogen (Fig. 7). Elevated $^{15}N/^{14}N$ isotope signatures may reflect the addition of nitrogen recycled from the downgoing slab, as suggested in the literature (Barry and Hilton, 2016; Bebout and Fogel, 1992; Busigny et al., 2003; Dauphas and Marty, 1999). To constrain whether subducted nitrogen is added to the sources of plumes and/or arc source, we make use of $N_2/^{36}Ar$ and $N_2/^{3}He$ ratios.

7. Coupling $^{15}N^{15}N$ and ^{36}Ar data: important but challenging

The ratios N_2/Ar and $N_2/^{36}Ar$ are used routinely as tracers of volatile origin, and are also important data for calculating fluxes of N_2 outgassing. Published $N_2/^{36}Ar$ data with Δ_{30} values are shown on Fig. 5 and the significance of the potential correlations are discussed in the following section. We also present combinations of Δ_{30} data with $^{40}Ar/^{36}Ar$ (Fig. 6) and discuss the intricacies of the ^{36}Ar-N_2 geochemical pair, as revealed by $^{15}N^{15}N$ data.

7.1 Using $^{15}N^{15}N$ to determine $N_2/^{36}Ar$ ratios

433 The first important observation on Fig. 5 is that at atmospheric Δ_{30}, $N_2/^{36}Ar$ ratios are
434 variable. They range from the nominal value for air of ~$2.5x10^4$ to~$0.4x10^4$. The low end of
435 the range is three times below the anticipated $N_2/^{36}Ar$ for air-saturated waters of ~$1.2x10^4$.
436 This is likely the result of hydrothermal degassing described in section 6. The solubilities of
437 argon and nitrogen are distinct by about a factor of 2 in geothermal waters, at temperatures
438 between 20 and 100 °C (Ballentine et al., 2002). Assuming hydrothermal degassing occurs
439 as a Rayleigh distillation process, and using the solubility relationships reviewed in
440 Ballentine et al., (2002), 95% N_2 degassing would be associated with 75% Ar degassing,
441 causing $N_2/^{36}Ar$ of the residual fluids to be fractionated (lowered) by a factor of ~3 relative
442 to the starting composition (Labidi et al., 2021). The discovery that degassing fractionates
443 N_2/Ar ratios is important with respect to the use of nitrogen excesses, N_2*, introduced by
444 Fischer et al., (1998). Excess nitrogen is defined as $[N_2^*] = [N_2]_{measured} - 40 \times [Ar]_{measured}$. The
445 numerical value 40 corresponds to the N_2/Ar ratio of air-saturated water. It is an important
446 notion, used to pro-rate the bulk flux of N_2 to obtain the volcanic fraction only, in entire arcs
447 (Fischer et al., 2002). Any $N_2/Ar > 40$ is thought to reflect the contribution of volcanic
448 nitrogen with high N_2/Ar added to unfractionated air-saturated waters. The prospect that
449 atmospheric components in fact have variable N_2/Ar likely warrants revisiting the notion of
450 N_2*.

451 The relationships between $N_2/^{36}Ar$ and Δ_{30} can be projected to high-temperature
452 endmembers with Δ_{30} = 0‰, to estimate the $N_2/^{36}Ar$ ratio of the volcanic gases. Yellowstone
453 fumaroles characterized by air-like $N_2/^{36}Ar$ span nearly the entire range of Δ_{30} values (Fig.
454 5A). However, having taken into account the variable degrees of elemental fractionation of
455 air prior to mixing, the Yellowstone dataset is reasonably consistent with a high $N_2/^{36}Ar$ of

~10^6, similar to MORB (Fig. 5A). Fumaroles from the Central America subduction zone are far more ambiguous. The data distribution can be fit with a high-temperature endmember with $N_2/^{36}Ar$ anywhere between ~10^6 (similar to MORB, Fig. 5A) and ~10^4 (similar to air, fig. 5B). These ratios have vastly different implications for the volatile budget and fluxes in a subduction zone. The ambiguity results from the curvature in Δ_{30} – $N_2/^{36}Ar$ space. For mixtures between air and MORB-like gases, mixing hyperbolae are associated with considerable curvature. Most of the curvature occurs where $\Delta_{30} < \sim 4$ (Fig. 5A), such that for any $\Delta_{30} > 4$, gas mixtures will inevitably be biased towards the $N_2/^{36}Ar$ of air. This means that unless Δ_{30} of a mixed gas is almost indistinguishable from the high-temperature endmember, which is a rare occurrence, the $N_2/^{36}Ar$ ratio remains poorly constrained by Δ_{30} – $N_2/^{36}Ar$ extrapolations.

7.2 Constraints from $^{40}Ar/^{36}Ar$ ratios

A novel way to independently constrain $N_2/^{36}Ar$ ratios of high-temperature endmembers is to plot Δ_{30} directly against $^{40}Ar/^{36}Ar$ (Fig. 6). In this space, samples from intra-plate volcanism (Eifel and Yellowstone) show correlations which confirm that argon and N_2 act essentially as geochemical pairs in hydrothermal fluids. Mixing curvatures are defined by $[^{14}N^{14}N/^{36}Ar]_{Mantle}/[^{14}N^{14}N/^{36}Ar]_{Air}$. Taking the $N_2/^{36}Ar$ ratio for air-saturated water and $^{40}Ar/^{36}Ar$ of both air (~300) and the plume endmembers (~30,000 for Eifel, ~10,000 for Yellowstone, see detail in Labidi et al., 2020), a simple data fit returns the $N_2/^{36}Ar$ for the volcanic endmember. Overall, Yellowstone data are fit with a $N_2/^{36}Ar$ between $0.3^{+0.2}_{-0.1} \times 10^6$ and $1.0^{+0.6}_{-0.4} \times 10^6$ for the plume endmember (Fig. 6A). This is striking because again, $N_2/^{36}Ar$ of individual samples are much closer to air (section 7.1). This

exercise would be valuable for fumaroles in a subduction zone, since it could distinguish whether $N_2/^{36}Ar$ ratios for sub-arc source is 10^6 or 10^4 (Fig. 5A versus 5B). However, arc fumaroles from Central America have atmospheric $^{40}Ar/^{36}Ar$ values even for near-zero Δ_{30} values, so a spectrum of scenarios may account for the data. An endmember possibility is that the sub-arc mantle sources have $^{40}Ar/^{36}Ar \sim 25{,}000$, i.e. the value of the upper mantle away from direct slab influences (Moreira et al., 1998). To fit the vertical relationship in figure 6, the required $N_2/^{36}Ar$ would have to be $\sim 10^8$ (Fig. 6B). In this case, the sub-arc mantle would have to receive subducted nitrogen but no slab-derived argon at all, hence a high $N_2/^{36}Ar$ and a MORB-like $^{40}Ar/^{36}Ar$. This may appear as unreasonable. In addition, arguments based on $^3He/^{36}Ar$ suggest the addition of ^{36}Ar to sub-arc sources is actually significant, which argues against a $N_2/^{36}Ar$ ratio of $\sim 10^8$ (Labidi et al., 2021). Instead, the sub-arc mantle may be overwhelmed with atmospheric argon, with $^{40}Ar/^{36}Ar \sim 300$. In this scenario, the $N_2/^{36}Ar$ of the arc source can be anything, but the vertical relationship on Fig. 6 is explained by volcanic argon having atmospheric $^{40}Ar/^{36}Ar$ ratios. This scenario is consistent with the notion of subduction barrier for light noble gases (Moreira, 2013; Moreira and Raquin, 2007; Staudacher and Allègre, 1988). It would incidentally confirm that as opposed to Δ_{30} data, the Ar isotope systematic is not a strong tracer of air contamination in arc regions, since high-temperature volatiles would have argon isotope compositions similar to air.

8. Determining the sources of N in the mantle

A quantification of the flux of slab-derived N_2 to mantle sources is necessary for understanding Earth's nitrogen cycle. Assuming that ^3He subduction is negligible (Porcelli et

al., 2002), the combination of $N_2/^3He$ ratios and Δ_{30} values provides a particularly powerful approach. For a discussion on $^3He/^{22}Ne$ and $^3He/^{36}Ar$ ratios, see Labidi et al., (2021). At Yellowstone, the data require a $N_2/^3He$ endmember of 3×10^6 (Fig. 4), indistinguishable from MORB. This $N_2/^3He$ estimate derived from Δ_{30} is the same as the lowest $N_2/^3He$ observed at Yellowstone by Chiodini et al. (2012). The MORB-like $N_2/^3He$ ratio for the high $^3He/^4He$ Yellowstone plume, confirmed using Δ_{30}, is an important observation. Every ^3He-rich mantle source may reflect a mixture of subducted and primordial reservoirs (Jackson et al., 2020) especially for heavy noble gases (Ballentine et al., 2005; Parai and Mukhopadhyay, 2018). Based on $^{15}N/^{14}N$ arguments, some have suggested the subducted components dominate the N budget of plume sources (Barry and Hilton, 2016; Bekaert et al., 2021; Marty and Dauphas, 2003). Following Sano et al., (2001), the subducted components would likely show extremely elevated $N_2/^3He$, perhaps as high as $\sim 10^{11}$. For subducted nitrogen to occur in the Yellowstone source but still account for a MORB-like $N_2/^3He$ ratio of the mantle plume, the primordial component would have to be characterized by an even lower $N_2/^3He$ ratios prior to slab addition. In Labidi et al., (2020), mixtures involving slabs with $N_2/^3He$ of 10^{11} were shown to require a primordial reservoir with $N_2/^3He \leq 2 \times 10^5$. A potential problem with this view is that the $N_2/^3He$ of Yellowstone gases of $\sim 10^6$ would result from mixing two extreme components in just the right proportions to yield convective mantle values. The homogeneous $N_2/^3He$ of $\sim 10^6$ between MORB and a plume would have to result from chance. A potentially simpler solution suggests that indistinguishable $N_2/^3He$ ratios for the convective and deep mantle reflect that subduction is not a major player at all for nitrogen in these reservoirs. The implications of the distinctive behaviors of nitrogen and heavy noble gases during subduction are discussed elsewhere (Labidi, in revision in this issue). As

described above, we can use the sample with the lowest Δ_{30} reported by Labidi et al. (2020) to provide a minimum $\delta^{15}N$ of ~+0.2‰ for Yellowstone mantle, similar to the $\delta^{15}N$ of ~0‰ for the Yellowstone endmember reported by Chiodini et al. (2012). Given that the $\delta^{15}N$ of 0.2 ‰ is a minimum value, it becomes clear that the high $^3He/^4He$ mantle source of Yellowstone features elevated $\delta^{15}N$ values yet with no resolvable N addition to the source (compared to a MORB mantle). We tentatively suggest that $\delta^{15}N \sim 0$‰ in plumes may be indigenous to the pristine mantle source rather than being the result of additions from descending slab material (Fig. 7).

Literature data from Iceland and the Azores fumaroles may have to be revisited in light of these findings. Fumaroles from these localities have $N_2/^3He$ values as low as ~10^7 that are associated with markedly negative $\delta^{15}N$ values (Marty et al., 1991; Caliro et al., 2015). It is tempting to attribute $\delta^{15}N \leq -10$‰ to a hint of primordial nitrogen in plumes, akin to the −20 ‰ to −47 ‰ $\delta^{15}N$ values exhibited by enstatite chondrites (Grady et al., 1986). However, the $N_2/^3He$ ratios of ~10^7 are still far removed from the MORB-like mantle endmember $N_2/^3He$ of ~3x10^6 that we obtain from Δ_{30}-$\delta^{15}N$ systematics for the high $^3He/^4He$ mantle at Yellowstone. Mixing between a mantle gas ($N_2/^3He$ ~10^6) and a relatively minute amount of fractionated air ($N_2/^3He$ ~10^{11}) can easily yield $N_2/^3He$ values ~10^7. A simple mass balance shows that any mixing proportion involving more than 1% of air increases the $N_2/^3He$ ratios to ~10^7 and overwhelms both Δ_{30} and $\delta^{15}N$ of the gas mixture air $\delta^{15}N$ values (e.g., Figure 4). Should $\delta^{15}N$ of that particular air component be mass fractionated, as we have shown is likely for air-derived nitrogen, $N_2/^3He$ ~10^7 will be observed together with low $\delta^{15}N$, leading us astray. We suggest this is the simplest explanation for the negative $\delta^{15}N$

signatures observed in Iceland (Marty et al., 1991) and the Azores (Caliro et al., 2015). Instead of explaining very low $\delta^{15}N$ values for the high $^{3}He/^{4}He$ mantle as vestiges of an enstatite chondrite source, we tentatively suggest that the high $^{3}He/^{4}He$ mantle may have a $\delta^{15}N$ slightly elevated compared to MORB, with values around ~0‰ or slightly higher (Fig. 7).

Eifel gases display $N_2/^{3}He$ ratios of 1.2 (±0.1) x10^{7} at near-zero Δ_{30} values (Fig. 4). This is about a factor of 2–4 times the value for MORB, supporting the notion of nitrogen addition to the Eifel mantle source. For gases from Central America, two-component mixing curves define mixing between air with $N_2/^{3}He$ ~10^{11} and high-temperature gases with $N_2/^{3}He$ ~10^{8} (Fig. 4). A $N_2/^{3}He$ ~10^{8}, higher than MORB by two orders of magnitude, is consistent with considerable nitrogen addition to sub-arc mantle sources (Labidi et al., 2021). Samples at Poás have negative $\delta^{15}N$, values associated with low N_2/He ratios (Fischer et al., 2002, Zimmer et al., 2004). This combination of geochemical features has been interpreted as resulting from contributions of gases from the upper mantle, suggested to account for ~80% of the vented N_2 (Fischer et al., 2002). However, these particular fumaroles have atmospheric Δ_{30} signatures (Labidi et al., 2021), which argues against a magmatic origin for N_2. Here again, the simplest explanation for the low N_2/He ratios may involve mixing between a mantle gas and air with fractionated $\delta^{15}N$ values. Importantly, the Δ_{30} data mitigates the need to invoke substantial MORB-like nitrogen within the Central American arc.

The new Δ_{30} data have been used to revisit the fluxes of nitrogen in arcs. Taking ^{3}He fluxes from the literature and a newly-defined $N_2/^{3}He$ ratios of ~ 10^{8}, Labidi et al. (2021) suggested N_2 outgassing fluxes are between 4.0 x 10^{8} and 1.0 x10^{9} mol N_2/y. The revised

nitrogen outgassing fluxes are comparable to the subduction flux of nitrogen in this subduction zone (Busigny et al., 2019). This suggests that in the Central American subduction zone, the subduction and volcanic degassing fluxes of nitrogen are in balance (Labidi et al., 2021), consistent with recent experimental work on the nitrogen partition coefficient between slabs and fluids (Jackson et al., 2021; Mallik et al., 2018). This in turn allows for the prospect that N_2 is quantitatively returned to the surface by degassing in subduction zones, precluding a net delivery of nitrogen to the deep mantle (Fig. 7). If this circumstance was typical globally and over geological timescales, it would explain the apparent contradiction that air has a higher $^{15}N/^{14}N$ than the mantle whereas delivery of isotopically heavy nitrogen in slabs to the mantle would predict the opposite over time. Relative isolation of the mantle nitrogen from the surface seems to be required over geological time scales (Labidi et al., 2020).

9. Concluding remarks

New Δ_{30} data, acquired with high-mass-resolution mass spectrometry, are a valuable tool to constrain the behavior and sources of nitrogen in natural gas mixtures. In hydrothermal fluids from various locations, the data are dominated by air-derived components rather than by high-temperature volcanic volatiles. Using these data, we find that air-derived components undergo isotope mass fractionations in hydrothermal systems. This leads to the emanation of air-derived gases with negative $\delta^{15}N$ values and anomalously low N_2/Ar and He/Ar ratios. This has consequence for the use of $\delta^{15}N$ and N_2/Ar as source tracers in hydrothermal gases.

593 The new Δ_{30} data have allowed determinations of mantle $\delta^{15}N$, $N_2/^{36}Ar$, and $N_2/^3He$
594 ratios beneath Eifel and Yellowstone. For Eifel, the mantle $N_2/^{36}Ar$ and $N_2/^3He$ values are
595 slightly greater than the values for the MORB mantle. These values may reflect the addition
596 of nitrogen via subduction in the Eifel source. At Yellowstone, the mantle $\delta^{15}N$, $N_2/^{36}Ar$, and
597 $N_2/^3He$ values determined with Δ_{30} data yield important information about the high $^3He/^4He$
598 mantle. The $N_2/^3He$ elemental ratio is indistinguishable from the MORB mantle, and thus
599 inconsistent with N addition to the high $^3He/^4He$ mantle. The $\delta^{15}N$ value is indistinguishable
600 from 0‰, after appropriate correction for air contamination. The new Δ_{30} data show that
601 suggestions of a high $^3He/^4He$ mantle with very negative $\delta^{15}N$ values are not warranted.
602 Instead, the observed low $\delta^{15}N$ values are the result of $^{15}N/^{14}N$ fractionation in hydrothermal
603 systems. Air-like $\delta^{15}N$ values with MORB-like $N_2/^3He$ ratios appear to be a fundamental
604 observation that constrains the origin of volatiles in the high $^3He/^4He$ mantle. More work is
605 needed on ^3He rich hotspots. Iceland hosts many fumaroles and geothermal wells where light
606 noble gases have features associated with the plume mantle (Füri et al., 2010). Acquisition
607 of Δ_{30} measurements for these fumaroles will be important. The only Δ_{30} measurements of
608 nitrogen from Icelandic fluids, reviewed here, have identified no non-atmospheric N_2. Future
609 attempts to identify high-temperature N_2 there, if successful, would be useful for
610 determining whether the low $N_2/^3He$ that characterizes the Yellowstone plume is a global
611 signature of the primordial mantle.

612 Plots featuring $^{40}Ar/^{36}Ar$ versus Δ_{30} are helpful when mantle endmembers have a known,
613 elevated, $^{40}Ar/^{36}Ar$ ratio, as in the cases of plumes. For those cases, measured $N_2/^{36}Ar$ on
614 individual samples are ambiguous regarding the source, but the approach of fitting mixing
615 curves to the data (e.g., Fig. 6) affords a determination of $N_2/^{36}Ar$. The approach is sensitive

to the $N_2/^{36}Ar$ ratios used for air components. When the $^{40}Ar/^{36}Ar$ of a mantle source is unknown (e.g., a subduction zone), the Δ_{30} data support the concept of sub-arc mantle sources entirely dominated by air-derived argon.

New Δ_{30} data provide novel constraints on the fate of nitrogen in subduction zones. The sub-arc source from the warm subduction zone in Central America is shown to have elevated $N_2/^3He$ by orders of magnitude compared to the MORB mantle. This shows considerable addition of N_2 to sub-arc sources. Revised fluxes in the Central American subduction zone are based on $N_2/^3He$ that in turn derive from the analysis of Δ_{30} data. The derived fluxes suggest that this margin is a subduction barrier for N_2. Using fluxes determined on warm subduction zones may be more relevant to the deep time than those characterizing cold subduction zones. The true influence of subduction on mantle volatiles through time warrants revision based on these results.

Appendix A: Mixing loops

The concept of isotope clumping uses the stochastic distribution of isotopologues as a reference frame. Mixing in this reference frame can be highly non-linear. We illustrate mixing with N_2 gases with different bulk isotopic composition, gas 1 with $\delta^{15}N$ of –200‰, and gas 2 with a $\delta^{15}N$ of +100‰. For this exercise, both gases will be assigned a stochastic distribution of isotopologues, i.e. Δ_{30} = 0‰. The stochastic relative abundance of $^{15}N^{15}N$ in gas 1 is the square of the singly-substituted value, treating relative abundances as probabilities:

$$x(^{15}N^{15}N)_{gas1} = x(^{15}N)^2 = 8.50 \times 10^{-6}, \quad (1)$$

where $x(^{15}N^{15}N)_{gas\ 1}$ is the mole fraction of the $^{15}N^{15}N$ isotopologue in gas 1, and so forth. Similarly, the stochastic relative abundance of $^{15}N^{15}N$ in gas 2 is:

$$x(^{15}N^{15}N)_{gas2} = x(^{15}N)^2 = 1.60 \times 10^{-5}. \quad (2)$$

We calculate the expected stochastic abundance of $^{15}N^{15}N$ for a 50:50 mixture of these two gases from the bulk $^{15}N/^{15}N$ ratio in the usual way, as the square of the bulk isotopic concentration

$$x(^{15}N^{15}N)_{50:50,stochastic} = x(^{15}N)^2 = 1.20 \times 10^{-5}. \quad (3)$$

However, simple mixing between these two gases does not involve bond rupture. Since molecules retain their original bond ordering, the physical mixture has an observed fractional abundance of $^{15}N^{15}N$ different from that in equation 3. The relative concentration of $^{15}N^{15}N$ for the physical mixture is

$$\frac{1}{2} x(^{15}N^{15}N)_{gas1} + \frac{1}{2} x(^{15}N^{15}N)_{gas2} = 1.23 \times 10^{-5} \quad (4)$$

Comparing the measured value from Equation (4) with the predicted stochastic value from Equation (3) leads to an apparent Δ_{30} value greater than zero:

$$\Delta_{30} = 10^3 (1.23 \times 10^{-5}/1.20 \times 10^{-5} - 1) = 25 ‰ \quad (5)$$

The mixing between these two gases results in a Δ_{30} value even higher than air. This effect may prove important for the interpretation of data on other planets or in the interstellar medium where cold chemistry will cause $^{15}N/^{14}N$ ratios to vary by extreme magnitudes in terrestrial terms (Füri and Marty, 2015). However on Earth, mixing between $^{15}N/^{14}N$ ratios differing by hundreds of per mil is unrealistic. Mixing between two gases with $\delta^{15}N$ of -10‰ and +10‰ encompasses the vast majority of likely scenarios on Earth. In this case, the mixing produces negligible effects. At a 50:50 mixture of gases with $\delta^{15}N$ values of -10‰ and +10‰ and Δ_{30} of 0‰, results in Δ_{30} value of 0.1‰. In other words, in mixing scenarios where $^{15}N/^{14}N$ ratios vary by less than ~ 40‰, the induced Δ_{30} values deviate from endmember values by at most tenths of per mil. We conclude that mixing in the Δ_{30} - $\delta^{15}N$ space where variations in $\delta^{15}N$ are less than many tens of per mil (e.g., Fig. 2) produces linear trends.

Appendix B: Combinatorial effects

The combinatorial effect is an artifact of the use of the stochastic reference frame to characterize enrichments and depletions of multiply-substituted isotopologues signatures (Taenzer et al., 2020; Yeung, 2016; Yeung et al., 2015; Young et al., 2017). It can arise where more than one isotopic pool of an element contributes to the formation of the multiply-substituted molecules of interest. The most succinct description of the effect is that the analyst can only measure the arithmetic mean of those distinct pools, in the form of the product molecules, whereas the actual abundance of the multiply-substituted, or "clumped", species is the result of the geometric mean. Here we dispense with the possibility that the difference between air and other reservoirs of N_2 might be the result of this effect.

We might imagine that N_2 molecules are constructed from two different sources of nitrogen with distinct $^{15}N/^{14}N$ ratios, $^{15}R_1$ and $^{15}R_2$. Such a circumstances may obtain in the construction of O_2 molecules during photosynthesis, for example (Yeung et al., 2015, Yeung 2016), or when adding H to CH_3 to form methane (Taenzer et al., 2020). In the case of the formation of a molecule with a stochastic abundance of $^{15}N^{15}N$, but in which $^{15}R_1$ and $^{15}R_2$ contribute to the two different positions in the homonuclear diatomic N_2, the ratio of $^{15}N^{15}N$ to $^{14}N^{14}N$, given as the ratio of their mole fractions, $x^{15}N^{15}N/x^{14}N^{14}N$, must be the probability of $^{15}R_1$ and $^{15}R_2$ occurring in the same molecule, or $^{15}R_1 \times ^{15}R_2$, so in reality $x^{15}N^{15}N/x^{14}N^{14}N = {}^{15}R_1 \times {}^{15}R_2$. However, the analyst has no *a prior* knowledge about the ratios $^{15}R_1$ and $^{15}R_2$. Therefore, when reporting Δ_{30} value for this gas, the only recourse available is to use the bulk $^{15}N/^{14}N$ of the molecules themselves to

derive the stochastic value (the denominator in Δ_{30} values). This bulk ratio is the arithmetic mean of the ratios $^{15}R_1$ and $^{15}R_2$, or $(^{15}R_1+^{15}R_2)/2$. The resulting expression for the "observed" Δ_{30} is

$$\Delta_{30} = \frac{x^{15}\mathrm{N}^{15}\mathrm{N} / x^{14}\mathrm{N}^{14}\mathrm{N}}{\left(\frac{^{15}\mathrm{R}_1 + ^{15}\mathrm{R}_2}{2}\right)^2} - 1 \qquad (6)$$

whereas the actual, "true" value should be

$$\Delta_{30} = \frac{x^{15}\mathrm{N}^{15}\mathrm{N} / x^{14}\mathrm{N}^{14}\mathrm{N}}{^{15}\mathrm{R}_1\,^{15}\mathrm{R}_2} - 1 \qquad (7)$$

where for convenience we have omitted the factor of 10^3 that puts the values in per mil. As an illustration, we consider the extreme case where the isotopic compositions of the two nitrogen pools differ by 100 ‰, a difference much greater than found among natural geochemical or biogeochemical reservoirs. In this example, $^{15}R_1 = 1.100 \times {}^{15}R_2$, or $\delta^{15}N_{(1)} = 100$‰ and $\delta^{15}N_{(2)} = 0$‰. In addition, for convenience, we stipulate that the "clumping" in this gas is 0, meaning that there is no excess in $^{15}N^{15}N$ relative to stochastic. Using the average natural abundances of ^{15}N and ^{14}N to define $^{15}R_2$, 0.00364 and 0.99636, respectively, we have $^{15}R_2 = 0.003653$, and the stochastic abundance of $^{15}N^{15}N$ in the N_2 composed of one atom from reservoir 1 and the other from reservoir 2 is $x^{15}N^{15}N/x^{14}N^{14}N = {}^{15}R_1 \times {}^{15}R_2 = 1.46812\times10^{-5}$. Using Equation (7) to calculate Δ_{30}, we obtain 0, as expected. However, the analyst cannot apply Equation (8) because there is nothing to indicate that the two nitrogen atoms represent two distinct isotopic pools; the values of $^{15}R_1$ and $^{15}R_2$ are unknowable. Forced to use Equation (6), the analyst obtains a Δ_{30} value of –2.27 ‰ for this stochastic gas. This is the spurious negative Δ value caused by the combinatorial effect. For more typical differences in $\delta^{15}N$ among relevant reservoirs of tens of per mil at most, these effects are on the order of a tenth of ‰ or less, and then only if N_2 is constructed from nitrogen atoms from two distinct isotopic pools. The combinatorial effect is not a factor in the applications described in this review, and it cannot explain the ~ 19 ‰ enrichment in $^{15}N^{15}N$ in air.

Appendix C: evidence against $^{15}N^{15}N$ bond re-ordering

Atmospheric N_2, with Δ_{30} ~19‰, may be kept at relatively high temperatures within heated hydrothermal systems. This could re-order nitrogen to a near-stochastic distribution of the doubly-substituted isotopologue $^{15}N^{15}N$, leading to N_2 with Δ_{30} =0. Partial or total bond re-ordering of atmospheric signatures is however considered unlikely, on the basis of experimental evidence and circumstancial observation in nature.

Pure N_2 at a pressure of 0.1 bar was heated at 800 °C for between 1 and 69 days. The heated N_2 yielded average Δ_{30} of 19.2±0.2 indistinguishable from the starting Δ_{30} composition of air. In a second set of experiments, N_2 was in contact with 2 grams of basalt powder (< 68 microns mesh), as a ways to increase the potential reaction surfaces between gases and solids with rock material that may be present at depths in natural hydrothermal systems. The gas+powder mixture was heated at 800 °C for up to 38 days. In these experiments N_2 yielded average Δ_{30} of 19.0±0.2.

The evidence against re-ordering in heating experiments is corroborated by circumstantial observations in nature. Gases vented at 400 °C in el Salvador, up to 212 °C in Iceland, and 200 °C in Hawaii are among the samples analyzed for Δ_{30} with the highest venting temperatures. At these temperature, bond re-ordering would result equilibrium Δ_{30} value below 0.3‰ (Yeung et al., 2017). However, nitrogen from these samples have high Δ_{30} value of 15.5±0.3‰, 18.6±0.8‰ and 18.2±0.4‰ respectively. Those are near atmospheric signatures which argues against the erasure of $^{15}N^{15}N$ atmospheric excesses. A number of other gases vented at ~100–150 °C show strictly atmospheric Δ_{30} values.

Last, we note that re-ordering would cause vertical trends in plots of Δ_{30} vs $\delta^{15}N$ on Figure 4, as it would only affect Δ_{30} values, not the bulk $^{15}N/^{14}N$ ratios. This is not observed; $^{15}N/^{14}N$ ratios correlate with Δ_{30} values. These correlations require mixing processes. The absence of Δ_{30} re-ordering on timescales relevant to hydrothermal systems allow extrapolation to $\Delta_{30} \sim 0$‰ to distinguish melt-derived volatiles from atmospheric components.

Captions

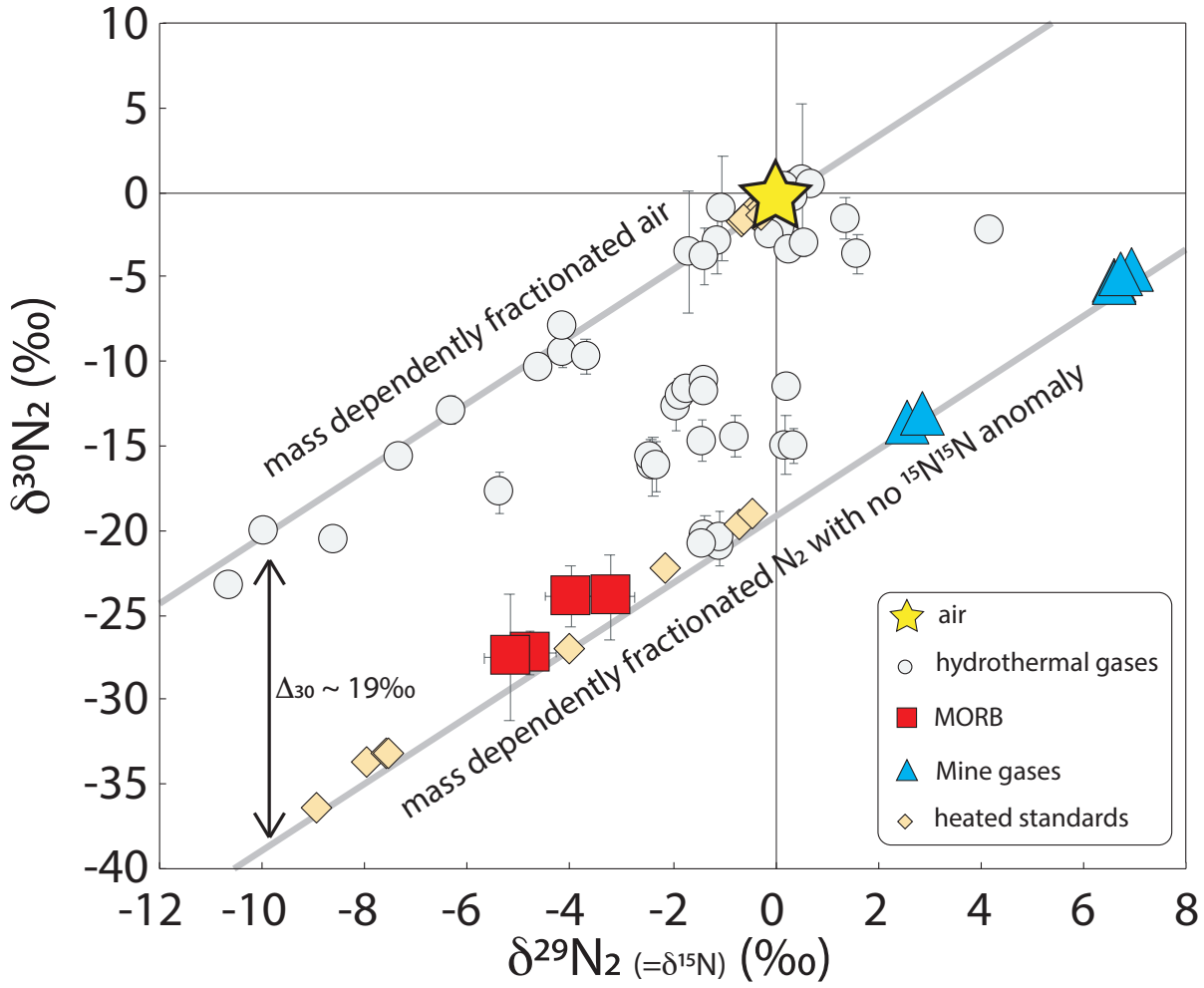

741

742 **Figure 1: Isotopic composition of N_2 from natural samples and laboratory experiments for $\delta^{30}N_2$ versus $\delta^{29}N_2$.** Mass-
743 dependent fractionation curves for air and high-temperature stochastic N_2 are shown. Data are from Yeung et al. (2017),
744 Labidi et al., (2020), and Labidi et al., (2021). Detail on heated gases can be found in Yeung et al., (2017). Briefly, heated
745 gases in the absence of a catalyst show un-equilibrated Δ_{30} values, so they plot near air. Only heated gases in the presence
746 of strontium nitride show re-ordered, stochastic distributions of $^{15}N^{15}N$. Most data on natural samples are from Labidi et
747 al., (2020, 2021). Natural samples are dominated by hydrothermal vents, but also include mid-ocean ridge basalts and mine
748 gases.
749
750
751

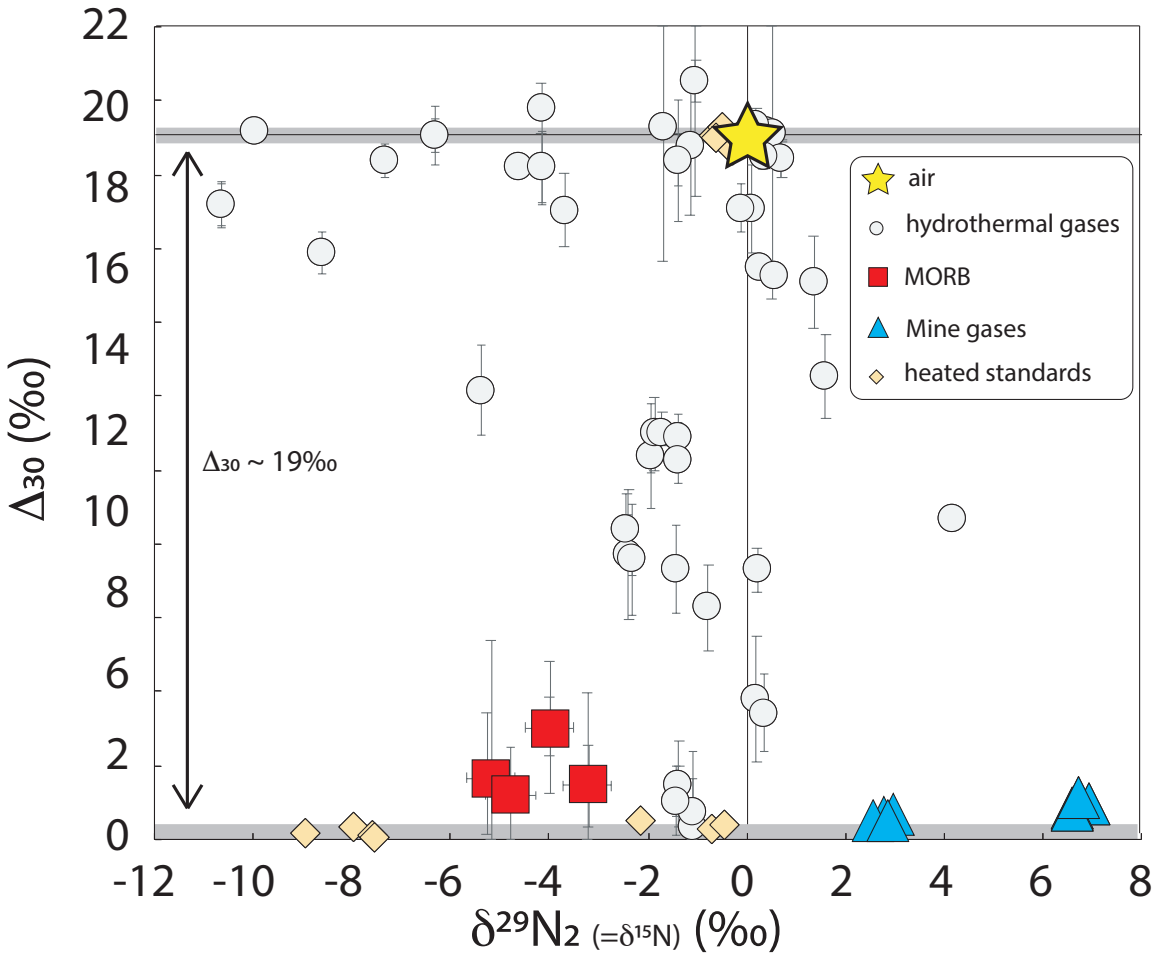

Figure 2: Isotopic composition of N_2 from natural samples and laboratory experiments for Δ_{30} versus $\delta^{15}N$. A ~19‰ offset is observed between air and stochastic gases. Hydrothermal samples show variable $\delta^{15}N$ and Δ_{30}. The Δ_{30} variation reflects mixing between stochastic and air-derived N_2. Importantly, negative $\delta^{15}N$ are almost exclusively associated with air that underwent N isotope fractionation, as shown by atmospheric Δ_{30} values.

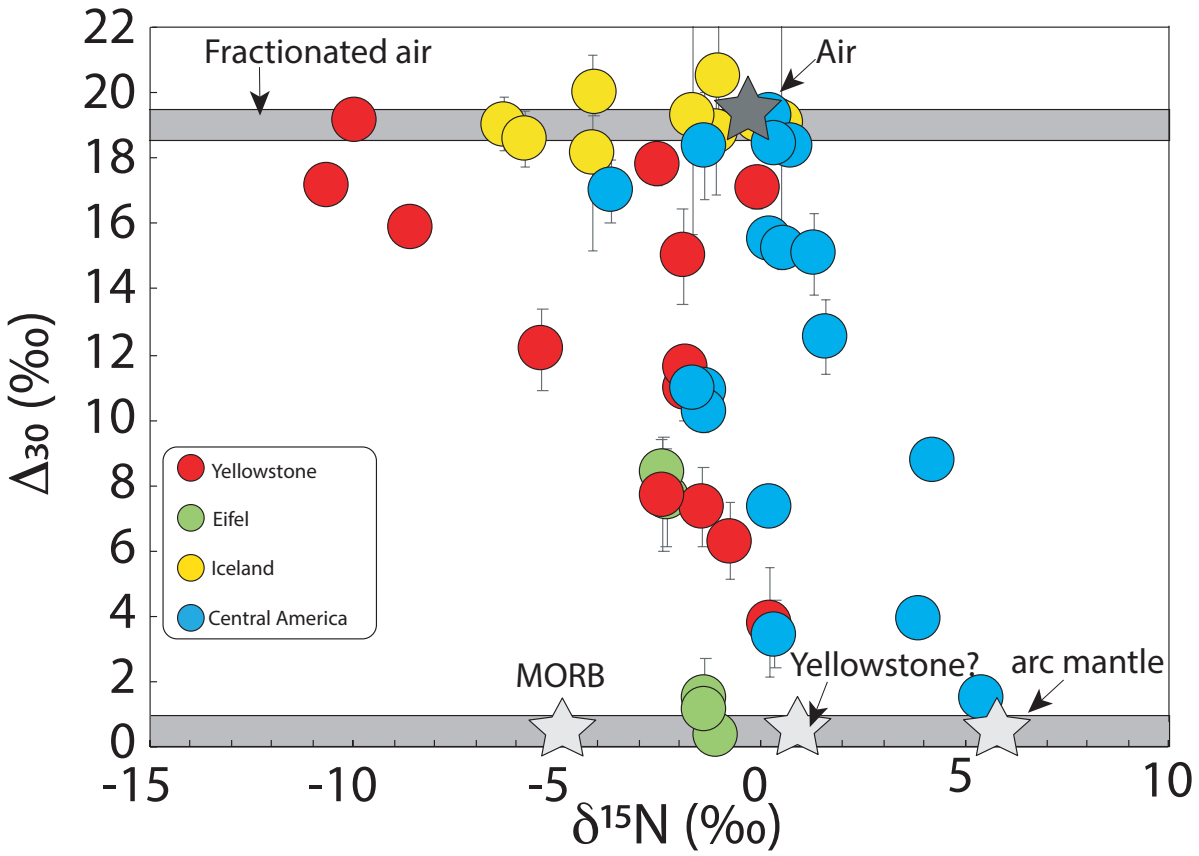

Figure 3: **nitrogen isotopic data of volcanic discharges from Iceland, Eifel, Yellowstone, and Central America**
Variable Δ_{30} values establish that the samples incorporate variable amounts of atmospheric nitrogen. At an air Δ_{30} value, variable $\delta^{15}N$ reflect a mass-dependent isotope fractionation associated with hydrothermal degassing. The high-temperature components are identified by attempting at extrapolating the trends. For Yellowstone, the scatter makes it particularly challenging, but the data appear consistent with a near-zero $\delta^{15}N$ value for the high-T endmember.

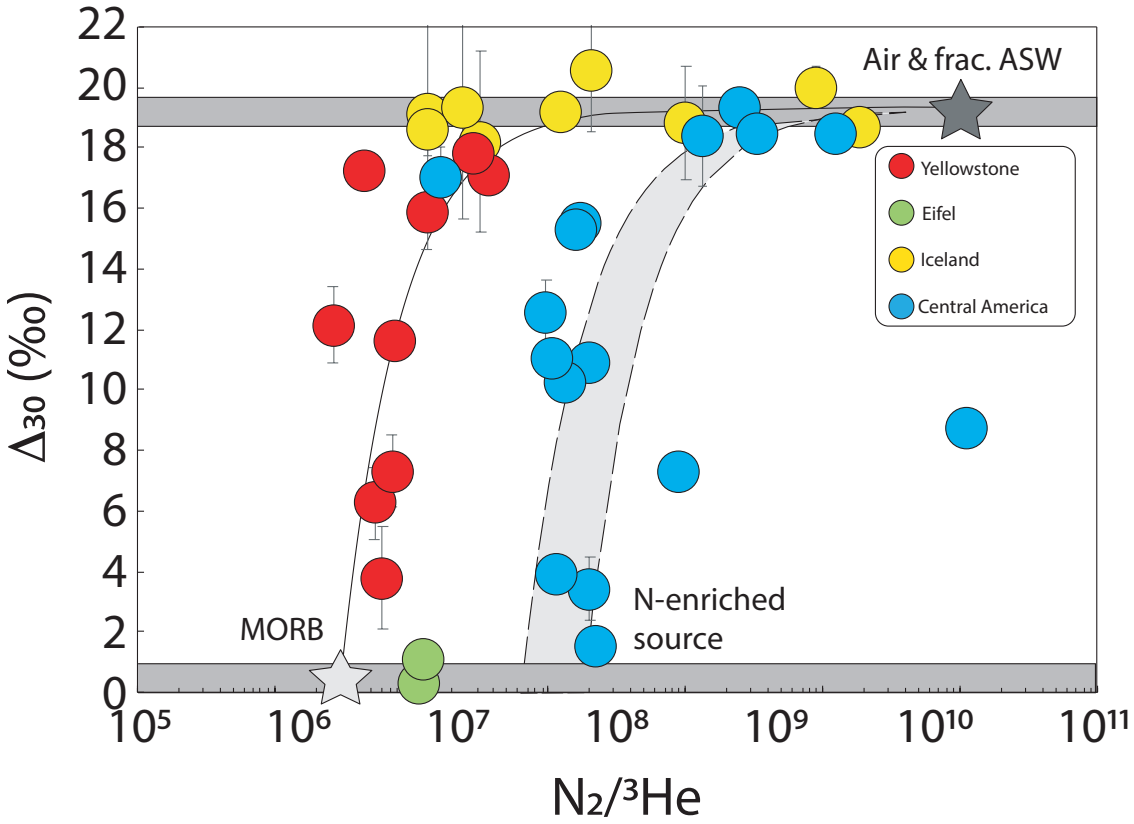

Figure 4: **Measured $N_2/^3He$ ratios versus Δ_{30} values.** Mixing lines are shown for mixtures between air and high temperature components. Because the solubility of N_2 and He are indistinguishable in waters at most hydrothermal temperatures (Ballentine et al., 2002), air, air-saturated water (ASW) and fractionated ASW all have indistinguishable $N_2/^3He$ ratios.

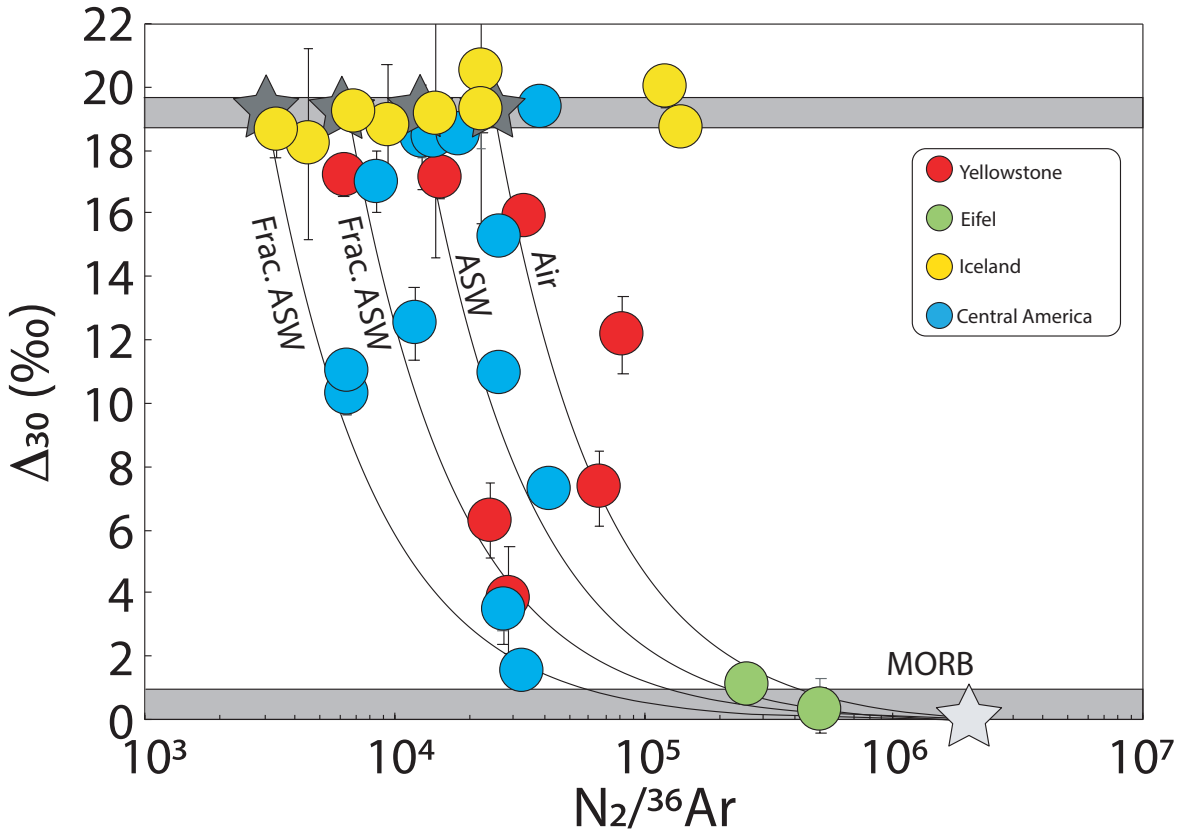
Yellowstone
Eifel
Iceland
Central America
Frac. ASW
Frac. ASW
ASW
Air
MORB
Δ30 (‰)
N2/36Ar

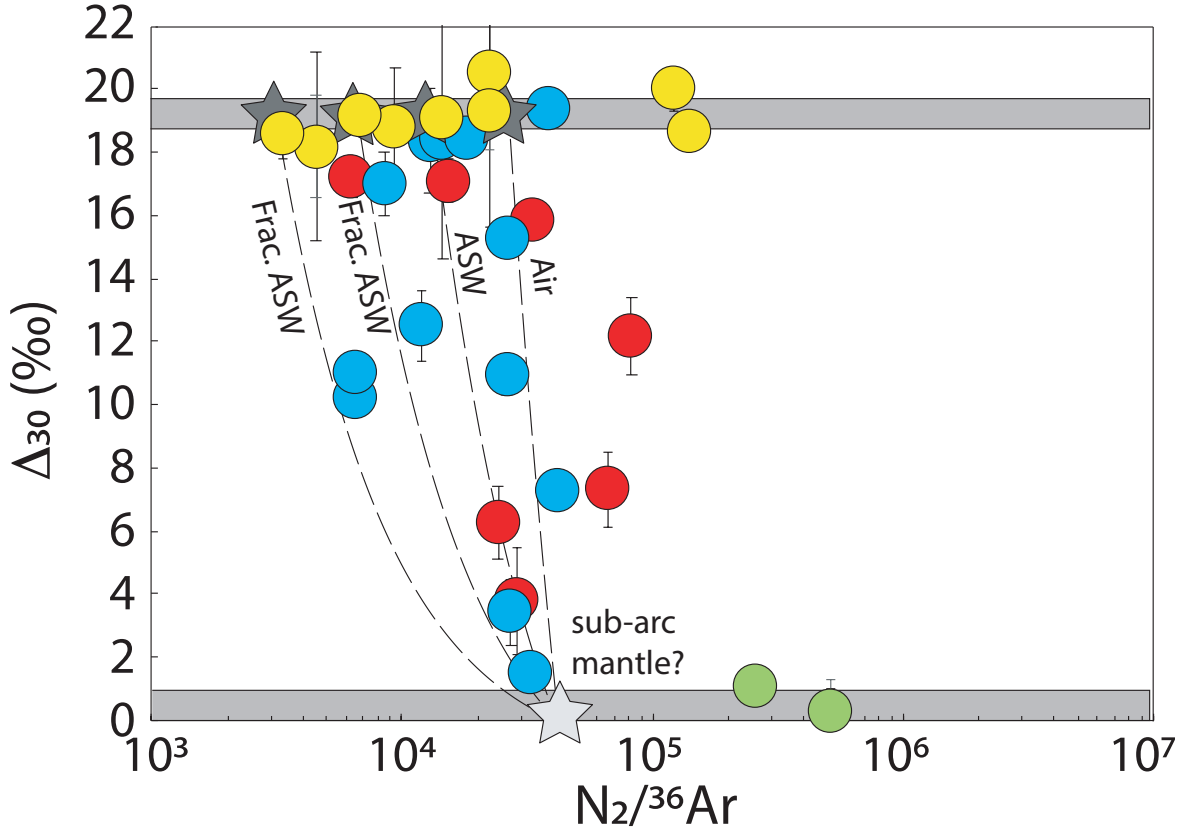
Frac. ASW
Frac. ASW
ASW
Air
sub-arc
mantle?
Δ30 (‰)
N2/36Ar

772

Figure 5: **Measured $N_2/^{36}Ar$ ratios versus Δ_{30} values.** Panel A and B are identical geochemical spaces with distinct mixing scenarios, constructed both in order to explain the Yellowstone and Central American data. In Panel A, mixing lines are between a MORB component and variably fractionated atmospheric components, including air, air-saturated water (ASW), and degassed water. In Panel B, mixing lines are between a hypothetical mantle wedge endmember and the same atmospheric components than in panel A.

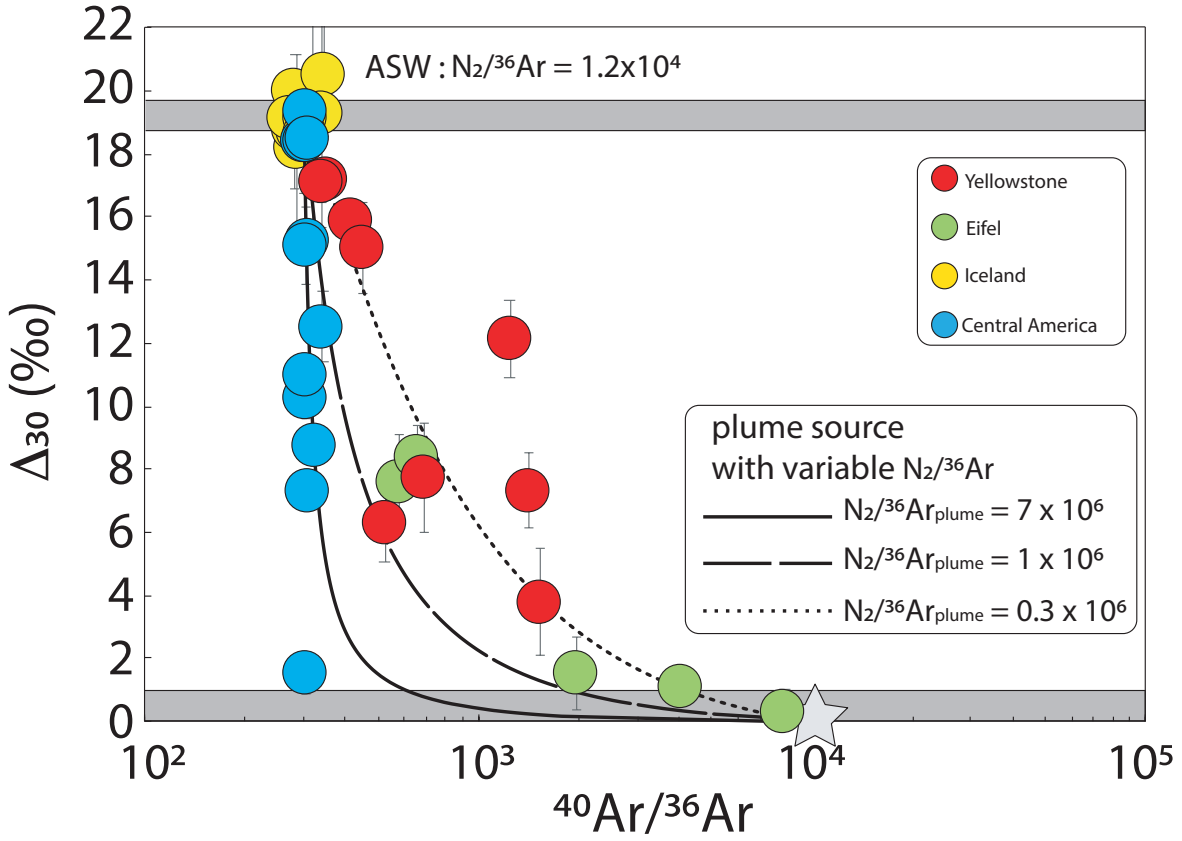
ASW : N2/36Ar = 1.2x10⁴
Yellowstone
Eifel
Iceland
Central America
plume source
with variable N2/36Ar
N2/36Arplume = 7 x 10⁶
N2/36Arplume = 1 x 10⁶
N2/36Arplume = 0.3 x 10⁶
Δ30 (‰)
40Ar/36Ar

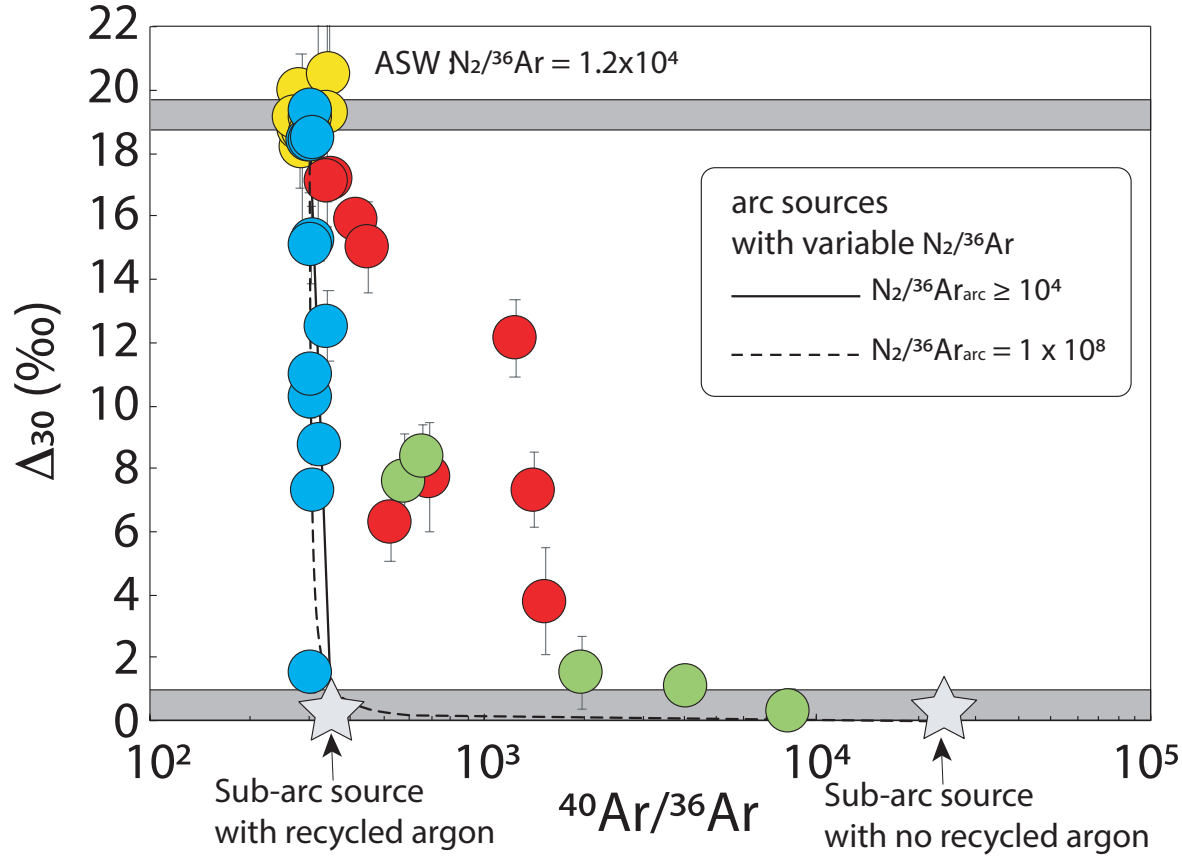
ASW N2/36Ar = 1.2x10⁴
arc sources
with variable N2/36Ar
N2/36Ararc ≥ 10⁴
N2/36Ararc = 1 x 10⁸
Δ30 (‰)
40Ar/36Ar
Sub-arc source
with recycled argon
Sub-arc source
with no recycled argon

779

Figure 6 **The relationship between nitrogen Δ_{30} and argon isotopes in volcanic gases**
Δ_{30} and $^{40}Ar/^{36}Ar$ ratios are shown for Iceland, Yellowstone, Eifel and central America gases. Panel A and B are identical geochemical spaces with distinct mixing scenarios. Panel A aims at accounting for the Yellowstone data. Mixing lines are between ASW and a hypothetical plume endmember with $^{40}Ar/^{36}Ar$ ratio of 10,000. Variable $N_2/^{36}Ar$ ratios for the plume component cause variable curvatures in the mixing relationships. Panel B aims at account for the Central American dataset. Mixing lines are between ASW and a hypothetical mantle wedge endmembers with variable $^{40}Ar/^{36}Ar$ ratios.

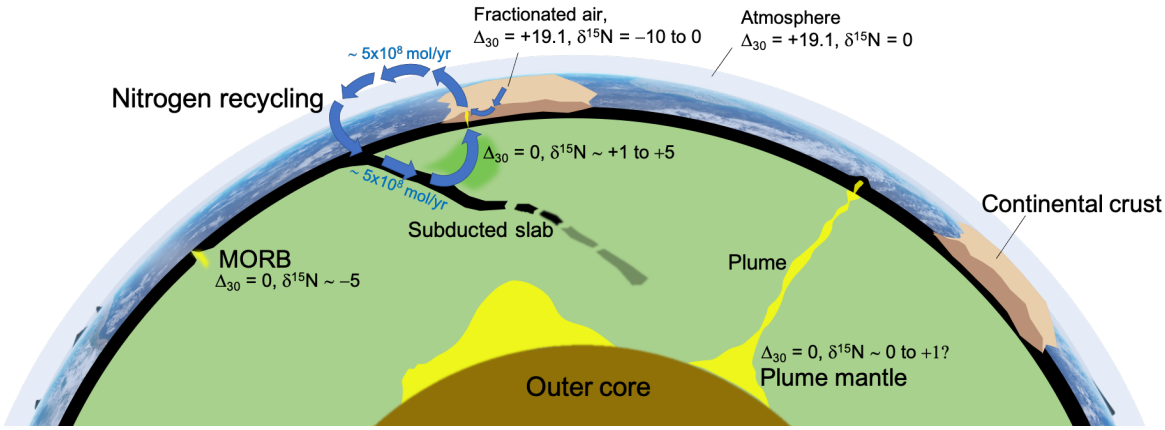

Figure 7 **Cartoon representing various processes and reservoirs constrained by $^{15}N^{15}N$ data.**
Not to scale. A section of Earth with the core, the mantle, the continental and oceanic crust, and the atmosphere are shown. A slab is shown to enter subduction. Air is the only reservoir with N_2 associated with a $^{15}N^{15}N$ anomaly of ~19‰. All other sources of N_2 have Δ_{30} ~ 0‰. The slab hosts nitrogen fixed as NH_4^+ (Busigny et al., 2019 and references therein) so no Δ_{30} values are defined; Δ_{30} is only relevant for N_2 molecules. Upon partial melting of a mantle source, magmatic N_2 would form with a Δ_{30} of 0‰. The high-T N_2 is then contributed to hydrothermal systems in the sub-surface by near-quantitative magmatic degassing. Air circulation in the sub-surface allows air-saturated waters to undergo degassing, and subsequent gas release with fractionated compositions. Plume data require a mantle source with a $\delta^{15}N$ ~0‰, from the study of Yellowstone, in agreement with Chiodini et al., (2012). No enstatite-like $\delta^{15}N$ signatures appear to be required by the data in the Yellowstone plume source. The plume source has a $N_2/^3He$ similar to the MORB mantle, which could challenge the notion of nitrogen addition to plume sources with elevated $^3He/^4He$ ratios (Labidi et al., 2020). The arc sources underneath the central American arc are even more enriched in $\delta^{15}N$, with values up to +5‰ according to $^{15}N^{15}N$ data. There, elevated $N_2/^3He$ across the entire arc require the overwhelming addition of surface-derived N to sub-arc sources. Recalculated fluxes suggest that, in that one subduction zone, ingassing and outgassing fluxes are matching within uncertainties (Labidi et al., 2021).

References

Ader, M., Thomazo, C., Sansjofre, P., Busigny, V., Papineau, D., Laffont, R., Cartigny, P., Halverson, G.P., 2016. Interpretation of the nitrogen isotopic composition of Precambrian sedimentary rocks: Assumptions and perspectives. Chem. Geol. 429, 93–110.

Ballentine, C.J., Burgess, R., Marty, B., 2002. Tracing fluid origin, transport and interaction in the crust. Rev. Mineral. geochemistry 47, 539–614.

Ballentine, C.J., Marty, B., Lollar, B.S., Cassidy, M., 2005. Neon isotopes constrain convection and volatile origin in the Earth's mantle.

Nature 433, 33–38.

Barry, P.H., Hilton, D.R., 2016. Release of subducted sedimentary nitrogen throughout Earth's mantle. Geochemical Perspect. Lett. 2, 148–159. https://doi.org/http://dx.doi.org/10.7185/geochemlet.1615

Bebout, G.E., Fogel, M.L., 1992. Nitrogen-isotope compositions of metasedimentary rocks in the Catalina Schist, California: implications for metamorphic devolatilization history. Geochim. Cosmochim. Acta 56, 2839–2849.

Bekaert, D.V., Turner, S.J., Broadley, M.W., Barnes, J.D., Halldórsson, S.A., Labidi, J., Wade, J., Walowski, K.J., Barry, P.H., 2021. Subduction-Driven Volatile Recycling: A Global Mass Balance. Annu. Rev. Earth Planet. Sci. 49.

Boudoire, G., Rizzo, A.L., Arienzo, I., Di Muro, A., 2020. Paroxysmal eruptions tracked by variations of helium isotopes: inferences from Piton de la Fournaise (La Réunion island). Sci. Rep. 10, 1–16.

Busigny, V., Cartigny, P., Philippot, P., 2011. Nitrogen isotopes in ophiolitic metagabbros: A re-evaluation of modern nitrogen fluxes in subduction zones and implication for the early Earth atmosphere. Geochim. Cosmochim. Acta 75, 7502–7521. https://doi.org/10.1016/j.gca.2011.09.049

Busigny, V., Cartigny, P., Philippot, P., Ader, M., Javoy, M., 2003. Massive recycling of nitrogen and other fluid-mobile elements (K, Rb, Cs, H) in a cold slab environment: evidence from HP to UHP oceanic metasediments of the Schistes Lustrés nappe (western Alps, Europe). Earth Planet. Sci. Lett. 215, 27–42. https://doi.org/10.1016/s0012-821x(03)00453-9

Caliro, S., Viveiros, F., Chiodini, G., Ferreira, T., 2015. Gas geochemistry of hydrothermal fluids of the S. Miguel and Terceira Islands, Azores. Geochim. Cosmochim. Acta 168, 43–57.

Cartigny, P., Jendrzejewski, N., Pineau, F., Petit, E., Javoy, M., 2001. Volatile (C, N, Ar) variability in MORB and the respective roles of mantle source heterogeneity and degassing: the case of the Southwest Indian Ridge. Earth Planet. Sci. Lett. 194, 241–257.

Chiodini, G., Caliro, S., Lowenstern, J.B., Evans, W.C., Bergfeld, D., Tassi, F., Tedesco, D., 2012. Insights from fumarole gas geochemistry on the origin of hydrothermal fluids on the Yellowstone Plateau. Geochim. Cosmochim. Acta 89, 265–278. https://doi.org/10.1016/j.gca.2012.04.051

Clayton, R.N., Mayeda, T., 1984. The oxygen isotope record in Murchison and other carbonaceous chondrites. Earth Planet. Sci. Lett. 67, 151–161.

Dauphas, N., Marty, B., 1999. Heavy nitrogen in carbonatites of the Kola Peninsula: A possible signature of the deep mantle. Science (80-.). 286, 2488–2490.

Elkins, L.J., Fischer, T.P., Hilton, D.R., Sharp, Z.D., McKnight, S., Walker, J., 2006. Tracing nitrogen in volcanic and geothermal volatiles from the Nicaraguan volcanic front. Geochim. Cosmochim. Acta 70, 5215–5235.

Fischer, T.P., Giggenbach, W.F., Sano, Y., Williams, S.N., 1998. Fluxes and sources of volatiles discharged from Kudryavy, a subduction zone volcano, Kurile Islands. Earth Planet. Sci. Lett. 160, 81–96.

Fischer, T.P., Hilton, D.R., Zimmer, M.M., Shaw, A.M., Sharp, Z.D., Walker, J.A., 2002. Subduction and recycling of nitrogen along the Central American margin. Science (80-.). 297, 1154–1157.

Fischer, T.P., Ramírez, C., Mora-Amador, R.A., Hilton, D.R., Barnes, J.D., Sharp, Z.D., Le Brun, M., de Moor, J.M., Barry, P.H., Füri, E., Shaw, A.M., 2015. Temporal variations in fumarole gas chemistry at Poás volcano, Costa Rica. J. Volcanol. Geotherm. Res. 294, 56–70. https://doi.org/10.1016/j.jvolgeores.2015.02.002

Füri, E., Hilton, D.R., Halldórsson, S.A., Barry, P.H., Hahm, D., Fischer, T.P., Grönvold, K., 2010. Apparent decoupling of the He and Ne isotope systematics of the Icelandic mantle: The role of He depletion, melt mixing, degassing fractionation and air interaction. Geochim. Cosmochim. Acta 74, 3307–3332. https://doi.org/10.1016/j.gca.2010.03.023

Füri, E., Marty, B., 2015. Nitrogen isotope variations in the Solar System. Nat. Geosci. 8, 515–522. https://doi.org/10.1038/ngeo2451

Füri, E., Portnyagin, M., Mironov, N., Deligny, C., Gurenko, A., Botcharnikov, R., Holtz, F., 2021. In situ quantification of the nitrogen content of olivine-hosted melt inclusions from Klyuchevskoy volcano (Kamchatka): Implications for nitrogen recycling at subduction zones. Chem. Geol. 120456.

Giggenbach, W.F., 1992. The composition of gases in geothermal and volcanic systems as a function of tectonic-setting, in: International Symposium on Water-Rock Interaction. pp. 873–878.

Grady, M.M., Wright, I.P., Carr, L.P., Pillinger, C.T., 1986. Compositional differences in enstatite chondrites based on carbon and nitrogen stable isotope measurements. Geochim. Cosmochim. Acta 50, 2799–2813.

Hashizume, K., Chaussidon, M., Marty, B., Robert, F., 2000. Solar wind record on the Moon: deciphering presolar from planetary nitrogen. Science (80-.). 290, 1142–1145.

Henkes, G.A., Passey, B.H., Grossman, E.L., Shenton, B.J., Yancey, T.E., Pérez-Huerta, A., 2018. Temperature evolution and the oxygen isotope composition of Phanerozoic oceans from carbonate clumped isotope thermometry. Earth Planet. Sci. Lett. 490, 40–50.

Hilton, D.R., Fischer, T.P., Marty, B., 2002. Noble gases and volatile recycling at subduction zones. Rev. Mineral. geochemistry 47, 319–370.

Jackson, C.R.M., Cottrell, E., Andrews, B., 2021. Warm and oxidizing slabs limit ingassing efficiency of nitrogen to the mantle. Earth Planet. Sci. Lett. 553, 116615.

Jackson, M.G., Blichert-Toft, J., Halldórsson, S.A., Mundl-Petermeier, A., Bizimis, M., Kurz, M.D., Price, A.A., Harðardóttir, S., Willhite, L.N., Breddam, K., 2020. Ancient helium and tungsten isotopic signatures preserved in mantle domains least modified by crustal recycling. Proc. Natl. Acad. Sci. 117, 30993–31001.

Jambon, A., 1994. Earth degassing and large-scale geochemical cycling of volatile elements. Volatiles in magmas 479–518.

Javoy, M., 1998. The birth of the Earth's atmosphere: the behaviour and fate of its major elements. Chem. Geol. 147, 11–25.

Javoy, M., Pineau, F., 1991. The volatiles record of a "popping" rock from the Mid-Atlantic Ridge at 14°N: chemical and isotopic composition of gas trapped in the vesicles. Earth Planet. Sci. Lett. 107, 598–611.

Labidi, J., Barry, P.H., Bekaert, D. V, Broadley, M.W., Marty, B., Giunta, T., Warr, O., Lollar, B.S., Fischer, T.P., Avice, G., 2020. Hydrothermal 15 N 15 N abundances constrain the origins of mantle nitrogen. Nature 580, 367–371.

Labidi, J., Young, E.D., Fischer, T.P., Barry, P.H., Ballentine, C.J., de Moor, J.M., 2021. Recycling of nitrogen and light noble gases in the Central American subduction zone: constraints from 15N15N. Earth Planet. Sci. Lett.

Lee, H., Sharp, Z.D., Fischer, T.P., 2015. Kinetic nitrogen isotope fractionation between air and dissolved N2 in water: Implications for hydrothermal systems. Geochem. J. 49, 571–573.

Li, L., Bebout, G.E., 2005. Carbon and nitrogen geochemistry of sediments in the Central American convergent margin: Insights regarding subduction input fluxes, diagenesis, and paleoproductivity. J. Geophys. Res. Solid Earth 110.

Li, L., Li, K., Giunta, T., Warr, O., Labidi, J., Lollar, B.S., 2021. N2 in deep subsurface fracture fluids of the Canadian Shield: Source and

889 possible recycling processes. Chem. Geol. 120571.
890 Mallik, A., Li, Y., Wiedenbeck, M., 2018. Nitrogen evolution within the Earth's atmosphere–mantle system assessed by recycling in
891 subduction zones. Earth Planet. Sci. Lett. 482, 556–566.
892 Marty, B., 1995. Nitrogen content of the mantle inferred from N2–Ar correlation in oceanic basalts. Nature 377, 326.
893 Marty, B., Chaussidon, M., Wiens, R.C., Jurewicz, A.J.G., Burnett, D.S., 2011. A 15N-poor isotopic composition for the Solar System as shown
894 by Genesis solar wind samples. Science (80-.). 332, 1533–1536.
895 Marty, B., Dauphas, N., 2003. The nitrogen record of crust–mantle interaction and mantle convection from Archean to Present. Earth
896 Planet. Sci. Lett. 206, 397–410. https://doi.org/10.1016/s0012-821x(02)01108-1
897 Marty, B., Gunnlaugsson, E., Jambon, A., Oskarsson, N., Ozima, M., Pineau, F., Torssander, P., 1991. Gas geochemistry of geothermal fluids,
898 the Hengill area, southwest rift zone of Iceland. Chem. Geol. 91, 207–225.
899 Marty, B., Humbert, F., 1997. Nitrogen and argon isotopes in oceanic basalts. Earth Planet. Sci. Lett. 152, 101–112.
900 Marty, B., Zimmermann, L., 1999. Volatiles (He, C, N, Ar) in mid-ocean ridge basalts: Assesment of shallow-level fractionation and
901 characterization of source composition. Geochim. Cosmochim. Acta 63, 3619–3633.
902 Marty, B., Zimmermann, L., Pujol, M., Burgess, R., Philippot, P., 2013. Nitrogen Isotopic Composition and Density of the Archean
903 Atmosphere. Science (80-.). 342, 101–104. https://doi.org/10.1126/science.1240971
904 Moreira, M., 2013. Noble gas constraints on the origin and evolution of Earth's volatiles. Geochemical Perspect. 2, 229–230.
905 Moreira, M., Kunz, J., Allegre, C., 1998. Rare gas systematics in popping rock: isotopic and elemental compositions in the upper mantle.
906 Science (80-.). 279, 1178–1181.
907 Moreira, M., Raquin, A., 2007. The origin of rare gases on Earth: The noble gas 'subduction barrier'revisited. Comptes Rendus Geosci. 339,
908 937–945.
909 Mukhopadhyay, S., 2012. Early differentiation and volatile accretion recorded in deep-mantle neon and xenon. Nature 486, 101–104.
910 https://doi.org/10.1038/nature11141
911 Parai, R., Mukhopadhyay, S., 2018. Xenon isotopic constraints on the history of volatile recycling into the mantle. Nature 560, 223.
912 Parai, R., Mukhopadhyay, S., Tucker, J.M., Pető, M.K., 2019. The emerging portrait of an ancient, heterogeneous and continuously evolving
913 mantle plume source. Lithos 346, 105153.
914 Pedroni, A., Hammerschmidt, K., Friedrichsen, H., 1999. He, Ne, Ar, and C isotope systematics of geothermal emanations in the Lesser
915 Antilles Islands Arc. Geochim. Cosmochim. Acta 63, 515–532.
916 Pinti, D.L., Hashizume, K., Matsuda, J., 2001. Nitrogen and argon signatures in 3.8 to 2.8 Ga metasediments: Clues on the chemical state of
917 the Archean ocean and the deep biosphere. Geochim. Cosmochim. Acta 65, 2301–2315.
918 Porcelli, D., Ballentine, C.J., Wieler, R., 2002. An Overview of Noble Gas Geochemistry and Cosmochemistry. Rev. Mineral. geochemistry
919 47, 1–19. https://doi.org/10.2138/rmg.2002.47.1
920 Roulleau, E., Sano, Y., Takahata, N., Kawagucci, S., Takahashi, H., 2013. He, N and C isotopes and fluxes in Aira caldera: comparative study
921 of hydrothermal activity in Sakurajima volcano and Wakamiko crater, Kyushu, Japan. J. Volcanol. Geotherm. Res. 258, 163–175.
922 Sano, Y., Fischer, T.P., 2013. The analysis and interpretation of noble gases in modern hydrothermal systems, in: The Noble Gases as
923 Geochemical Tracers. Springer, pp. 249–317.

924 Sano, Y., Takahata, N., Nishio, Y., Fischer, T.P., Williams, S.N., 2001. Volcanic flux of nitrogen from the Earth. Chem. Geol. 171, 263–271.
925 Sano, Y., Takahata, N., Nishio, Y., Marty, B., 1998. Nitrogen recycling in subduction zones. Geophys. Res. Lett. 25, 2289–2292.
926 Sano, Y., Urabe, A., Wakita, H., Chiba, H., Sakai, H., 1985. Chemical and isotopic compositions of gases in geothermal fluids in Iceland.
927 Geochem. J. 19, 135–148.
928 Snyder, G., Poreda, R., Hunt, A., Fehn, U., 2001. Regional variations in volatile composition: Isotopic evidence for carbonate recycling in
929 the Central American volcanic arc. Geochemistry, Geophys. Geosystems 2.
930 Staudacher, T., Allègre, C.J., 1988. Recycling of oceanic crust and sediments: the noble gas subduction barrier. Earth Planet. Sci. Lett. 89,
931 173–183.
932 Taenzer, L., Labidi, J., Masterson, A.L., Feng, X., Rumble III, D., Young, E.D., Leavitt, W.D., 2020. Low Δ12CH2D2 values in microbialgenic
933 methane result from combinatorial isotope effects. Geochim. Cosmochim. Acta 285, 225–236.
934 Taran, Y.A., 2011. N 2, Ar, and He as a tool for discriminating sources of volcanic fluids with application to Vulcano, Italy. Bull. Volcanol.
935 73, 395–408.
936 Taran, Y.A., 2009. Geochemistry of volcanic and hydrothermal fluids and volatile budget of the Kamchatka–Kuril subduction zone.
937 Geochim. Cosmochim. Acta 73, 1067–1094.
938 Trieloff, M., Kunz, J., Clague, D.A., Harrison, D., Allègre, C.J., 2000. The nature of pristine noble gases in mantle plumes. Science (80-.). 288,
939 1036–1038.
940 Vaselli, O., Tassi, F., Minissale, A., Montegrossi, G., Duarte, E., Fernandez, E., Bergamaschi, F., 2003. Fumarole migration and fluid
941 geochemistry at Poás volcano (Costa Rica) from 1998 to 2001. Geol. Soc. London, Spec. Publ. 213, 247–262.
942 Williams, C.D., Mukhopadhyay, S., 2018. Capture of nebular gases during Earth's accretion is preserved in deep-mantle neon. Nature 565,
943 78–81. https://doi.org/10.1038/s41586-018-0771-1
944 Yeung, L.Y., 2016. Combinatorial effects on clumped isotopes and their significance in biogeochemistry. Geochim. Cosmochim. Acta 172,
945 22–38.
946 Yeung, L.Y., Ash, J.L., Young, E.D., 2015. Biological signatures in clumped isotopes of O2. Science (80-.). 348, 431–434.
947 Yeung, L.Y., Li, S., Kohl, I.E., Haslun, J.A., Ostrom, N.E., Hu, H., Fischer, T.P., Schauble, E.A., Young, E.D., 2017. Extreme enrichment in
948 atmospheric 15N15N. Sci. Adv. 3, eaao6741.
949 Young, E.D., Galy, A., Nagahara, H., 2002. Kinetic and equilibrium mass-dependent isotope fractionation laws in nature and their
950 geochemical and cosmochemical significance. Geochim. Cosmochim. Acta 66, 1095–1104.
951 Young, E.D., Kohl, I.E., Lollar, B.S., Etiope, G., Rumble Iii, D., Li, S., Haghnegahdar, M.A., Schauble, E.A., McCain, K.A., Foustoukos, D.I., 2017.
952 The relative abundances of resolved 12CH2D2 and 13CH3D and mechanisms controlling isotopic bond ordering in abiotic and
953 biotic methane gases. Geochim. Cosmochim. Acta 203, 235–264.
954 Zimmer, M.M., Fischer, T.P., Hilton, D.R., Alvarado, G.E., Sharp, Z.D., Walker, J.A., 2004. Nitrogen systematics and gas fluxes of subduction
955 zones: insights from Costa Rica arc volatiles. Geochemistry, Geophys. Geosystems 5.
956
957
958

959
960
961
962
963